Volume 6
Number 3
7 February 2024
Pages 735–1026

Nanoscale Advances

rsc.li/nanoscale-advances

ISSN 2516-0230

ROYAL SOCIETY OF CHEMISTRY

PAPER

Wendel Wohlleben, Stefania Sabella *et al.*
Critical aspects in dissolution testing of nanomaterials in the oro-gastrointestinal tract: the relevance of juice composition for hazard identification and grouping

NCNST

Nanoscale Advances

ROYAL SOCIETY OF CHEMISTRY

PAPER

View Article Online
View Journal | View Issue

Check for updates

Cite this: *Nanoscale Adv.*, 2024, **6**, 798

Critical aspects in dissolution testing of nanomaterials in the oro-gastrointestinal tract: the relevance of juice composition for hazard identification and grouping†

Luisana Di Cristo,§[a] Johannes G. Keller,‡[b] Luca Leoncino,[c] Valentina Marassi,[d] Frederic Loosli,[be] Didem Ag Seleci,[b] Georgia Tsiliki,[f] Agnes G. Oomen,[gi] Vicki Stone,[h] Wendel Wohlleben *[b] and Stefania Sabella *[a]

The dissolution of a nanomaterial (NM) in an *in vitro* simulant of the oro-gastrointestinal (OGI) tract is an important predictor of its biodurability *in vivo*. The cascade addition of simulated digestive juices (saliva, stomach and intestine), including inorganic/organic biomacromolecules and digestive enzymes (complete composition, referred to as "Type 1 formulation"), strives for realistic representation of chemical composition of the OGI tract. However, the data robustness requires consideration of analytical feasibility, such as the use of simplified media. Here we present a systematic analysis of the effects exerted by different digestive juice formulations on the dissolution% (or half-life values) of benchmark NMs (*e.g.*, zinc oxide, titanium dioxide, barium sulfate, and silicon dioxide). The digestive juices were progressively simplified by removal of components such as organic molecules, enzymes, and inorganic molecules (Type 2, 3 and 4). The results indicate that the "Type 1 formulation" augments the dissolution *via* sequestration of ions by measurable factors compared to formulations without enzymes (*i.e.*, Type 3 and 4). Type 1 formulation is thus regarded as a preferable option for predicting NM biodurability for hazard assessment. However, for grouping purposes, the relative similarity among diverse nanoforms (NFs) of a NM is decisive. Two similarity algorithms were applied, and additional case studies comprising NFs and non NFs of the same substance were included. The results support the grouping decision by simplified formulation (Type 3) as a robust method for screening and grouping purposes.

Received 2nd August 2023
Accepted 7th November 2023

DOI: 10.1039/d3na00588g

rsc.li/nanoscale-advances

Open Access Article. Published on 08 December 2023. Downloaded on 2/2/2024 12:01:41 PM.
This article is licensed under a Creative Commons Attribution-NonCommercial 3.0 Unported Licence.

1 Introduction

When ingested, a nanomaterial (NM) undergoes diverse physical, chemical, and biological transformations within the oro-gastro-intestinal (OGI) tract as a consequence of interactions with the surrounding environment (*e.g.*, digestive juices, pH, *etc.*).[1] For many ingested NMs, dissolution is an example of chemical transformation which may result in instantaneous, quick, gradual or very slow release of soluble molecular species (*i.e.*, ions) and/or particles with reduced or increased size than the original NMs (*i.e.* agglomerates).[2] The measurement of NM 'dissolution kinetics' may assess quantitatively the contribution of ions *vs.* particles and link this to the likelihood of bio-persistence of nanospecific properties (*i.e.*, the retention of the nanoscale size) as well as their potential accessibility to systemic circulation *in vivo*. Hence, dissolution can potentially be considered a predictor parameter of hazards[2–5] and its determination is recently included as part of the minimum requirements for NMs needed from a regulatory point of view.[4,6] For instance, if a NM undergoes complete dissolution quickly,

[a]*Istituto Italiano Di Tecnologia, Nanoregulatory Group, D3PharmaChemistry, Genova, Italy. E-mail: stefania.sabella@iit.it*

[b]*Department of Material Physics and Department of Experimental Toxicology and Ecology, BASF SE, Ludwigshafen, Germany. E-mail: wendel.wohlleben@basf.com*

[c]*Electron Microscopy Facility, Istituto Italiano di Tecnologia, Genova, Italy*

[d]*Department of Chemistry "G. Ciamician", University of Bologna, Italy*

[e]*University of Vienna, Vienna, Austria*

[f]*Institute for the Management of Information Systems, Athena Research Center, Marousi, Greece*

[g]*National Institute for Public Health and the Environment (RIVM), Bilthoven, The Netherlands*

[h]*Institute of Biological Chemistry, Biophysics and Bioengineering, Heriot-Watt University, Edinburgh, UK*

[i]*University of Amsterdam, Amsterdam, The Netherlands*

† Electronic supplementary information (ESI) available. See DOI: https://doi.org/10.1039/d3na00588g

§ Present address: GSK, Siena, Italy.

‡ Present address: Procter & Gamble Service GmbH, Sulzbacher Str. 40-50, 65824 Schwalbach am Taunus.

© 2024 The Author(s). Published by the Royal Society of Chemistry

Open Access Article. Published on 08 December 2023. Downloaded on 2/2/2024 12:01:41 PM. This article is licensed under a Creative Commons Attribution-NonCommercial 3.0 Unported Licence.

this results in generation of ions or molecules, and therefore the toxicity expected corresponds to those of the dissolved species; thus, it can be assessed by conventional risk assessment (RA).[4] In contrast, when the NM does not dissolve completely, both ions and particles may contribute to NM toxicity that may be related either to local damage to the intestinal epithelia/microbiota or systemic toxicity due to accumulation in secondary organs.[2] To quantitatively identify when the dissolution can be considered complete or incomplete, recent studies have proposed experimental cut-off values. For example, the European Food Safety Authority (EFSA) identified complete dissolution when 12% or less of the initial mass of the digested material is found in nanosized forms upon more than 30 minutes of intestinal digestion (corresponding to 155 minutes of incubation in the simulant intestine, reported as Int_1 within the manuscript). Moreover, to aid data harmonization, the EFSA suggests expressing dissolution kinetics as half-life ($t_{1/2}$) values which are measured according to the ISO 19057:2017.[4] In particular, the EFSA establishes $t_{1/2} \leq 10$ min (as measured at Int_1) as an inclusion criterion for instantaneously dissolving nanoforms (NFs), showing that particles dissolving in less than 10 min are unlikely to persist for long enough to cross the gastrointestinal mucus layer and to reach the enterocytes. The EU project GRACIOUS further specified the spectrum of cut-offs identifying intermediate temporal states ranging from quick to gradual or very slow dissolution. Here the framework additionally introduced 2 h and 60 h as second and third cut-off values, to define the boundaries for quick ($t_{1/2} > 10$ min and ≤ 2 h), gradual ($t_{1/2} > 2$ h and ≤ 60 h) or slow dissolving NFs ($t_{1/2} > 60$ h). These pragmatic cut-offs are experimentally derived and considered physiologically relevant to reflect whether constituent ions or molecules, particles or both contribute to toxicity. The application of these cut-offs allows for grouping NFs according to their persistence in the OGI tract.[2] Overall, the assessment of dissolution generally is associated with tiered toxicity testing to account for the hazard of both ions and particles.[2,4]

Being a kinetic process, dissolution is sensitive to many intrinsic and extrinsic parameters. Intrinsic parameters affecting dissolution include the digestive juices and all conditions mimicking the temporal evolving status of human digestion (*i.e.*, temperature, pH values, volumes of the digestive compartments and gradual release of digestive components *e.g.*, bile salts, enzymes, foods and so forth). Intrinsic parameters assessed *in vitro* must use standardized methods as much as possible to reduce variability. For instance, it has been demonstrated that the acidic pH of the dissolution medium is the primary factor responsible for accelerating the dissolution of zinc oxide (ZnO) NMs.[7] During digestion, food molecules may also interact with NFs *via* complexation, thus possibly impacting the dissolution/bioavailability of NMs. Available data on ZnO NFs demonstrate that the digestion under fed (*e.g.* in the presence of food additives such as starch, milk, oil and mix) or under fasting conditions does not greatly differ. In the presence of food, a stabilization effect on particle size rather than a real impact on dissolution has been noted;[8] even in the case of titanium dioxide (TiO_2) NFs, it has been demonstrated that the presence of a food matrix does stabilize the NF suspension, acting as a good dispersant during each digestive phase, thus preserving the original size of the NM.[9]

Extrinsic parameters relevant to dissolution kinetics are the physical chemical (PC) properties of the NMs, which can be applied to group NFs of a NM with similar properties.[2,3,10–14]

Currently, different *in vitro* methods are available to measure dissolution, in static or dynamic mode (*e.g.*, flow-through and continuous flow), as described by the ISO/TR 19057.[5] The molecular composition of the simulated juices usually varies in regard to the extent of prediction of *in vivo* conditions when a toxicity assessment is required. Generally, the presence of key components (enzymes, organic acids, foods of different chemical compositions such as sugars or lipids, *etc.*) can influence the bioavailability of molecules or nanoparticles (*via* dissolution or complexation), especially if they are poorly soluble (as is the case of metal derived NFs *e.g.* TiO_2 NFs). Many juices (FaSSGF/FeSSGF and FaSSIF/FeSSGF) either simulating fasting or fed conditions are available in the literature.[15–17] Validated or standardized simulant digestive formulations (*e.g.* DIN/ISO 19738 or NanoREG juices referred to in the manuscript as DIN and NR, respectively) are currently accessible from ISO documents and/or the EU project derived SOP (*e.g.*, NaNoREG "A common European approach to the regulatory testing of nanomaterials" D2.08 SOP 06, ISO/TR 19057 and Deutsches Institut fur Normung E.V., DIN/ISO 19738). These juices are very similar to FaSSGF or FaSSIF which are normally applied in drug pharmaceutics[16] although with minor changes (for example the presence or absence of inorganic salts, related concentration and albumin). Such juices have been widely used for NM digestion.[2,8,18–21]

The "cascade *in vitro* digestion assay" is acknowledged as the most popular static assay, which simulates the passage of the NF within the OGI tract under fasting conditions through the sequential addition of simulated saliva, stomach and intestine.[2,8,19,22–24] This assay allows the dissolution kinetics of NFs in semi-realistic environments (cascade addition of biomacromolecules and salts simulating the molecular compositions of the digestive juices and drastic changes in pH values and digestive volumes according to human physiology) to be studied.[25] Recently, by using the cascade *in vitro* digestion assay, the dissolution% of silver nanomaterials (Ag NMs) in OGI simulant juices was measured; moreover, the amount of bio accessible soluble silver ions in the intestine compartment was quantified and compared with the amount of silver in the faeces and blood of rats which were treated with comparable doses of NPs. The findings demonstrated a good match between *in vitro*/*in vivo* quantified ions highlighting the *in vivo* predictivity of the test.[18] More data (including dose–response) are needed to properly substantiate *in vitro–in vivo* predictivity of the cascade assay; however, the few pieces of evidence indicate its potential in applications addressing hazard assessment and/or grouping. Recently, advanced *in vitro* digestive assays (initially implemented for food digestion or for microbiota analysis) have been under evaluation to study the dissolution of NMs under conditions as much as possible predictive of an *in vivo* scenario.[17,26]

Open Access Article. Published on 08 December 2023. Downloaded on 2/2/2024 12:01:41 PM. This article is licensed under a Creative Commons Attribution-NonCommercial 3.0 Unported Licence.

While the cascade based digestive method has found many applications, the simulating fluids (intended as the molecular composition of each ingredient) to be applied are subject to open debate. In fact, there is still no common decision (which might include scientific justification) on which juice formulations to use. Here, the main differences in the juice simulants available are related to the extent of physiological molecular representativeness, *e.g.*, from very simple compositions (*i.e.*, only the acidic or neutral pH of a digestion step) to rather complex mixtures to simulate GI fluids, including digestive enzymes, bile salts, foods, salts, and lecithin (*e.g.* under fasting or fed conditions).[4]

According to the EFSA guideline, a rationale for the selection of digestive juice formulations and *in vitro* digestion assays should aim at representing physiological exposure (*e.g.*, ingestion).[4] Moreover, the reliability and reproducibility of the model should be assessed and documented. For instance, complex fluids with high concentrations of enzymes or NFs are challenging in post digestion-analysis treatments due to problems associated with aggregation or precipitation phenomena.[27] Thus, on considering the analytical issues that can occur, there is an urgent need to simplify the juice composition while trying to maintain a certain level of test predictivity. Furthermore, the rationale for the choice of simulant juice should be driven by the research need. Here, more relevant physiological methods could be required to demonstrate that a specific NF fulfils the EFSA criteria of quick dissolution, whereas if the goal of the research is a comparative screening of high numbers of NFs, the use of complex media might slow down the entire analysis or impede a high throughput screening.

In either case, the trade-offs between being realism and robustness must be considered. One purpose that requires comparative screening methods is grouping and read-across to allow a comparison of structurally related materials. According to the guidance of the European Chemicals Agency (ECHA),[6] by gathering similarities in PC and toxicological behaviour (mainly using *in vitro* screening methods), it is possible to substantiate a group of NFs for which the hazard assessment can be performed jointly for specific endpoints. A framework,[11] detailed guidance,[28] and an e-tool blueprint[29] were generated by the GRACIOUS project to support the endpoint-specific grouping of NFs. In addition, different human grouping hypotheses have been generated that take into consideration different routes of NF exposure, such as inhalation, and dermal and oral exposure, each with an adapted integrated approach to testing and assessment (IATA).[2,3,10,13] Here we focus on the methodology and cases studies to implement the IATA on oral hazards, where oral dissolution is a decisive decision node for the ensuing testing and assessment.

The aim of this work is the determination of relevant conditions to determine the dissolution kinetics (and thus the bioaccessibile ions for intestinal absorption) with a focus on the molecular composition of simulant digestive juices, that is defined as one of the complexities of the test. We apply a previously established method (the cascade method) using different simulant juices. We used a "Type 1 formulation" including the relevant organic, enzymatic and inorganic molecular components, as it is complete and the most physiologically representative. We progressively removed juice components to generate simplified sub-groups of juice formulations. This enabled us to identify the key "ingredients" that affect the trade-off of realism and robustness by modulating the measurable NF dissolution kinetics. In particular, we assessed the relevance of the enzymes in the juice composition *via* their impact on dissolution kinetics and on particle transformation by using four case studies, zinc oxide (ZnO), titanium dioxide (TiO_2), silicon dioxide (SiO_2) and barium sulphate ($BaSO_4$) NFs. We then applied an enzyme-free juice formulation (referred to as the Type 3 formulation) in a larger screening of case studies represented by different NFs and non-NFs and then used a similarity assessment to compare the results with the data obtained by the digestion with the Type 1 formulation. This exercise has led to the extrapolation of general criteria to define a suitable dissolution method for screening and supporting grouping, differentiating it from methods for hazard assessment.

2 Results and discussion

2.1 Rational design of sub-groups of simulant juice formulations (Type 1, 2, 3, and 4)

Scheme 1 underlines the digestive juice formulations selected in this study. The Type 1 formulation includes several molecular components that, for better clarity, we have classified as 'inorganic, organic/protein and enzymatic' molecular components. The Type 1 formulation is recognized as a more complete formulation in terms of ingredients with physiological representativeness. Such a formulation includes alpha (α)-amylase, pepsin, and other enzymes recognized to be relevant for chemical human digestion.[30–34] For instance, the α-amylase is involved in the cleavage of large starch molecules into maltose, ultimately yielding glucose. This enzyme has a relatively short active contact time with starch because once a food bolus is swallowed and infiltrated with gastric juice, its catabolic activity is mostly stopped by low acidic pH.[30] In the gastric juice, protein digestion is mostly taken over by the pepsin enzyme that is active under very acidic conditions (pH < 3.0), but becomes irreversibly inactivated above pH 5–6.[31,32] Finally, in the intestinal lumen, pancreatic lipase is one of the exocrine enzymes of pancreatic juice that is essential for digestion of dietary fats. This enzyme has an optimum pH of about 8.5 but is still very active at pH 6.5. The enzyme is irreversibly inactivated below pH 4.0.[33,34] Considerable amounts of albumin, bile salts (solubilizer of the products of lipase action)[35] and other organic and inorganic digestive components are also present.

In this work, we produced Type 1 formulations using biorelevant media over timeframes appropriate to gastrointestinal passage (0–245 minutes, depending on the digestive segment) in the absence of food components (fasting conditions). Although interactions with food components may have a role in stabilization of the colloidal suspension, thus influencing bioavailability and permeability of drug/NPs, herein, such conditions are not studied to reduce the array of experimental variables. We selected DIN and NR based juices as

 © 2024 The Author(s). Published by the Royal Society of Chemistry

Open Access Article. Published on 08 December 2023. Downloaded on 2/2/2024 12:01:41 PM.
This article is licensed under a Creative Commons Attribution-NonCommercial 3.0 Unported Licence.

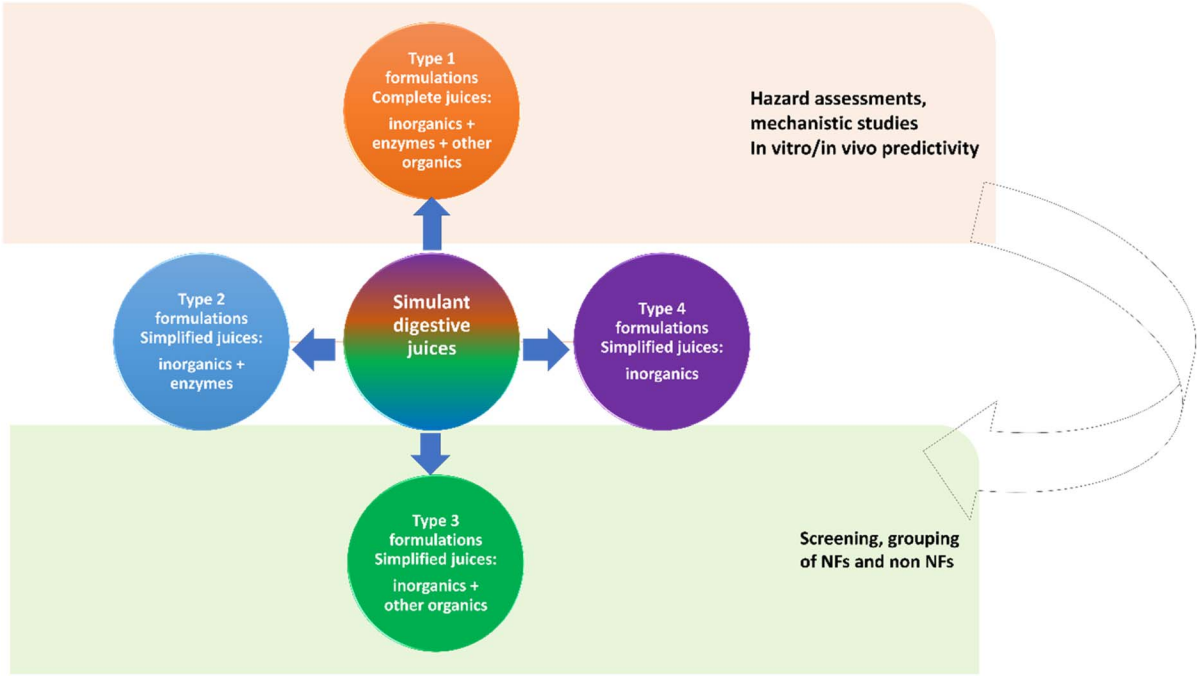

Scheme 1 Simulant digestive juices and relative formulations which were employed in the cascade *in vitro* digestion assay. The Type 1 formulation is referred to as "complete", and inorganics, organics/proteins and enzymatic ingredients are included. The Type 1 formulations can be considered as the most physiologically meaningful; they can be obtained by means of standard or validated simulant digestive juices (*i.e.* DIN ISO 19738 or NR juices). Type 1 formulations were progressively deprived of molecular ingredients to obtain simplified sub-groups, *i.e.*, Type 2, 3 and 4. Depending on the purpose of applications, a rational design of analytical criteria for dissolution testing is presented: for example, Type 1 formulations are preferable for hazard assessments, while Type 3 can be more suitable for screening or grouping of substances.

representatives of simulant OGI fluids. Emerging dissolution data on reference materials are currently available or under production by OECD by the use of these simulant juices, thus possibly aiding future benchmarking. In particular, NR juices were widely employed to study the dissolution of metal-like nanoparticles[2,18–20,22,36] and are currently under validation within the OECD Working Party on Manufactured Nanomaterials (WPMN) (ENV/CHEM/NANO(2019)5/ADD19).

Following the definition of a Type 1 formulation in Scheme 1, DIN and NR juices contain all the molecular components (inorganic, organic/protein and enzymatic ingredients), and hence are considered as 'complete' Type 1 formulations. However, it is important to underline that the two formulations are not identical with respect to the concentrations of some components (for instance, the lack of lipase and albumin in the DIN juice, makes it slightly simpler). We intentionally tested these different Type 1 juices to understand if minimal changes in molecular compositions will affect the dissolution rate.

Type 1 formulations were then progressively deprived of molecules to generate juice sub-groups as represented in Scheme 1. The Type 2 formulation consists of juice including 'inorganic and enzymatic molecular components', whereas Type 3 is completely depleted of the enzymatic ingredients. containing only the 'inorganic and organic/protein components'; finally, the Type 4 formulation includes only the inorganic molecular ingredients to ensure the pH values needed in the different steps of the digestion process. The detailed list of molecular components and relative concentrations applied is reported in Table S1–S3† which refer to the 'complete juice' (Type 1) and relative sub-groups (Type 2, 3, and 4) for both NR juices and DIN juices (for the latter, only Type 1 and 3 were prepared), respectively. These Type 2, 3 and 4 juices were used to assess the impact on dissolution kinetics of NMs exerted by the removal of entire molecular portions from the juice.

In this work, the dissolution of zinc oxide (ZnO), titanium dioxide (TiO_2), barium sulfate ($BaSO_4$) and silicon dioxide (SiO_2) NFs was assessed by employing the different juice type formulations. Other NFs and non NFs (ZnO, cerium dioxide (CeO_2) and some organic pigments) were also screened with the view to establish the use of simplified formulations (*i.e.* Type 3) to generate data suitable for grouping criteria (see the next section).

2.2 Dissolution of ZnO NFs by the cascade *in vitro* dissolution assay

2.2.1 Type 1 formulation (NR juices). Cascade *in vitro* dissolution assay was first operated using the Type 1 NR simulant juice and ZnO NFs. NM110 was selected as a representative example of ZnO NFs due to its extensive available characterization.[37] Fig. 1 and Table S4† report the % dissolution and the 'as measured ion' concentrations for NM110 (25–1000 mg L^{-1}) in the different digestive compartments (s, st, and int). In saliva (s), the % dissolution of NM110 is low but increases as the initial concentration of NM110 decreases,

Open Access Article. Published on 08 December 2023. Downloaded on 2/2/2024 12:01:41 PM.
This article is licensed under a Creative Commons Attribution-NonCommercial 3.0 Unported Licence.

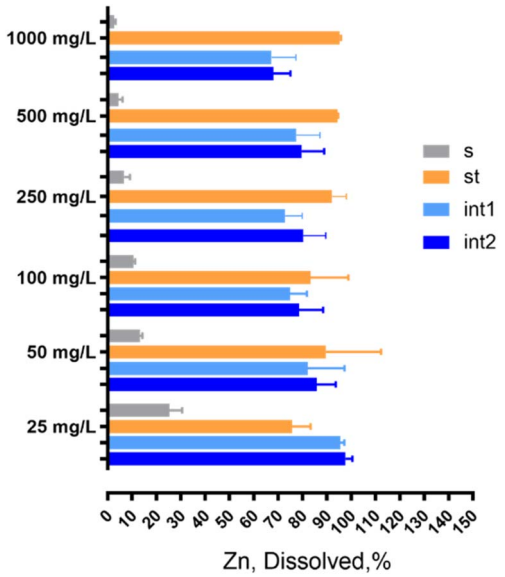

Fig. 1 Dissolution% of NM110 (ZnO) upon the application of the cascade *in vitro* digestion assay using the Type 1 formulation (NR juices). 25–1000 mg L^{-1} is the concentration range tested. Four temporal endpoints are measured which refer to the respective elapsed time of digestion in s (5 minutes), st (125 minutes) and int1 and int2 (after either 155 or 245 minutes of incubation). Data are measured by means of UF/ICP-OES (see 4.3.1.2 in the Experimental section) and expressed as average ± SD ($n \geq 3$). Data are reported as dissolved% values ($M_{ion}/M_0 \times 100$).

ranging from a minimum value of 2% (for 1000 mg L^{-1}) to a maximum of *ca.* 25% for the lower values (25 mg L^{-1}). In the stomach compartment (st), dissolution reaches *ca.* 80–100% in a dose independent manner (Fig. 1 and Table S4†). At the intestine level (int), the dissolution% is about 100% at the lower concentration employed (25 mg L^{-1}) but decreases down to *ca.* 70% for the highest concentrations (100–1000 mg L^{-1}) (Fig. 1 and Table S4†). This slight reduction of % dissolution provides evidence that, at pH values close to neutrality, the zinc ions (especially at concentrations above 50 mg L^{-1}) may precipitate at the intestinal site or further bio-transform upon specific interactions with the intestinal simulant molecular components, as also recently evidenced by Voss *et al.*[8] Overall, the presented results of this work are in line with recent findings reported by Sohal *et al.*,[22] showing a complete dissolution of ZnO NFs in the stomach and intestine environments. The dissolution values as measured at 155 minutes (Int1) can also be expressed as the dissolution rate, the half-life ($t_{1/2}$).[4,5] At the time of incubation, the $t_{1/2}$ of NM110 was below 5 minutes for a lower concentration but increased (hence the dissolution slowed down) to 30–60 minutes with increased NF concentration (Table S4†). Either way, these values classify NM110 as quick dissolving NFs in line with definition of the EFSA guideline and recent data reported by Di Cristo *et al.*[2,4]

2.2.1.1 Additional information on biotransformation of ZnO NFs by the multi-analytical approach (size distribution and chemical composition). The biotransformation of NM110 upon cascade addition of simulant OGI fluids was also followed by STEM-EDX analysis (Fig. S1†). In water, ZnO NFs appear as polydisperse sub-micron particles of various shapes and size of *ca.* 110 ± 60 nm (Fig. S2A†). The corresponding EDX spectrum confirms the presence of Zn by using the Zn-K_a peak (Fig. S1A†). After saliva incubation, the NFs are still visible although presenting smoother edges indicating that in saliva the dissolution of NM 110 occurs; however, we measured the size distribution of ZnO particles comparable to that obtained in water (Fig. S2B†) suggesting a dissolution relatively slower than that of the other digestive compartments (see below). The EDX analysis detects additional elements such as N, P, K Na and Cl, clearly referring to salts which are molecular ingredients of simulant saliva. In the stomach simulant fluid, no evidence of particles was found (Fig. S1C†) suggesting a very quick dissolution of the particles. A weak signal of Zn was found in one of the analyzed areas (see the black arrow in the inset of Fig. S1C†), but due to the extremely low signal, EDX mapping did not allow Zn localisation. Overall, the EDX results support the conclusions drawn by the dissolution data, showing the presence of distinct ZnO particles in the saliva compartment, and the almost or complete absence of particles in the stomach and in the intestine compartment, respectively (the latter is not shown). However, if particles were present, detection was very difficult under comparable conditions of analysis applied for the saliva sample.

Then FFF technique was applied to detect NFs by separation from the molecular components released during the dissolution. The experiments were conducted in FIA mode, either following injection of NM110 into the cascade *in vitro* digestion assay, or immediately after spiking known concentrations of NM110 into the single compartments prepared following the cascade addition of juices (*i.e.*, saliva, saliva plus stomach and saliva plus stomach plus intestine). Fig. S3† show the FIA signals and 3D spectra resulting from the consecutive protocol with or without NM110. Following a 5 minute digestion in the saliva simulant, the presence of nanoparticles is detected (Fig. S3A and B†). Saliva alone shows an absorption spectrum typical of proteins, with a local maximum at 280 nm but no absorption above this wavelength. In contrast, NM110 digested in saliva shows UV absorption that increases at both wavelengths (280 and 380 nm); in addition the spectrum shows an intense maximum at 380 nm that is typical for NM110.[38] Under the other two conditions tested (digestion in the stomach and intestine, Fig. S3C–F†) NFs were not detected, thus suggesting the complete dissolution of ZnO NFs immediately on the addition of stomach juice (Fig. S3C and D†). To improve the certainty that ZnO NFs dissolve totally in the stomach juice, NM110 was spiked directly into the stomach compartment (saliva/stomach cascade juice) to obtain a final concentration of 250 mg L^{-1} (ratio 1 : 1) (Fig. S4†). No signal for NFs was identified in the spectrum range of zinc adsorption under this condition, or for longer incubations of 2 h, or at higher concentrations (data not shown). However, it is possible that particles did remain undissolved but below the limit of detection (Fig. S5† reports the minimum concentration at which NM110 are visible in water by the same analytical method).

© 2024 The Author(s). Published by the Royal Society of Chemistry

Open Access Article. Published on 08 December 2023. Downloaded on 2/2/2024 12:01:41 PM.
This article is licensed under a Creative Commons Attribution-NonCommercial 3.0 Unported Licence.

2.2.2 Type 2, 3 and 4 formulations (NR juices). To systematically investigate the impact of the molecular composition of juice on dissolution of ZnO NFs, Type 2, 3 and 4 formulations employing NR juices (Table S2†) were applied in the cascade *in vitro* digestion assay and dissolution% measured upon NF incubation in the stomach and in the intestine juices (at an incubation time of 155 and 240 minutes, respectively). For sample collection, we selected these times as the *ca.* 70–100% of dissolution identified for NM110 by means of the Type 1 formulation (Fig. 1). Based on EFSA guidance, the concentrations of expected daily intake divided by 4 L of adult digestive juice volume are often too low for reliable analytical determination. As a compromise, we selected 50 mg L^{-1} as a representative concentration for which additional data on dissolution were collected by different groups.[2,13,18] The results (Fig. 2A) indicate that dissolution% of NM110 is comparable between Type 1 and 2 evidencing the null or slight role of the organic/protein component in promoting the dissolution of NM110. The most abundant components removed from Type 1 to obtain Type 2 include BSA, mucin and various bile components ranging from bile to glucuronic acid and so forth (Table S2†). Binding has been reported elsewhere between zinc ions and BSA or mucin. For example, mucins are reported to play a role in human intestinal zinc absorption,[39,40] and binding occurs at a molar ratio of 2 between the ion *vs.* the protein. However, under the experimental conditions applied in this work, the data presented here clearly indicate that such ingredients do not contribute to the key mechanisms (*e.g.* ion sequestration) affecting dissolution of metal containing materials (see the results below for the Type 3 formulation). While bile salts are known to be stabilizers of colloidal suspensions,[35,41] these components did not determine changes in the dissolution efficiency of ZnO under the conditions applied herein.

In contrast, when the enzymatic molecular components were removed completely to generate the Type 3 formulation, the dissolution drastically decreased in the simulated intestine compartment (Fig. 2A), reaching *ca.* 50–60% at the end of the process (int2 time point). The same trend is maintained when we measured the dissolution rate (expressed as half-life values), where the half-life goes from about 30 minutes to *ca.* 140 minutes at Int1 (namely after 30 minutes of intestinal incubation) and, finally, reaches *ca.* 450 minutes at the end of the digestion simulated process (data not shown). Interestingly, these results suggest that NM110 dissolution is influenced by enzyme content.

To provide insights on the mechanism of action, the concentration of the enzymatic molecular components (overall enzyme content) of the Type 1 formulation was progressively reduced to 70, 50 and 25% and down to 0% (this latter point corresponds to the Type 3 formulation), where the enzymes were absent. As shown in Fig. 2B, the gradual reduction of the enzyme concentration induced a significant decrease in the % dissolution in the intestinal compartment of about 40%. These data indicate that the presence of enzymes (all employed during human digestion) is needed to obtain a complete dissolution of ZnO NFs; we attribute this observation to an enzyme mediated zinc ion sequestration that impacts dissolution kinetics, promoting further dissolution.

We have already reported evidence that zinc ion sequestration by interactions with bio-macromolecules plays a role in dissolution in a sweat simulant fluid containing the amino acid histidine.[13] By blocking the coordination binding sites of histidine with cobalt ions, it has been demonstrated that histidine plays a direct role in enhancing the dissolution of ZnO NFs by sequestration of Zn^{2+} ions.[13]

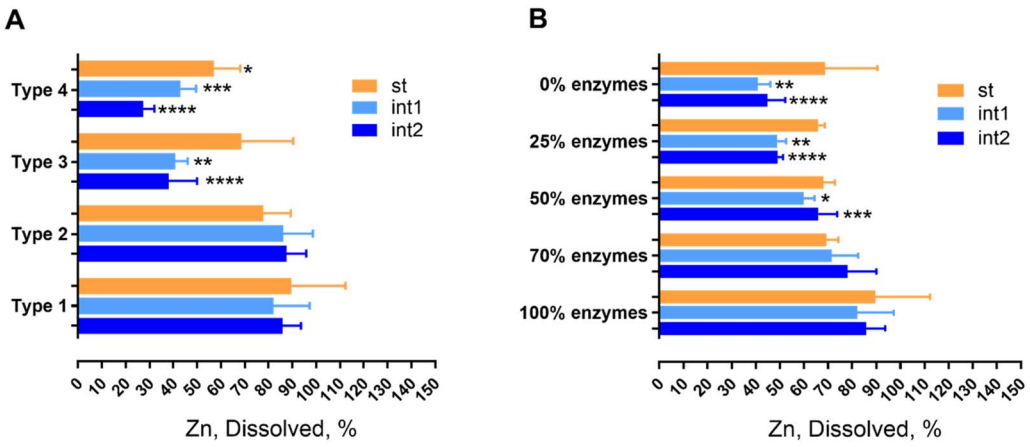

Fig. 2 (A) Dissolution of NM110 (50 mg L^{-1}) upon the application of the cascade *in vitro* digestion assay in formulation Type 1, Type 2, Type 3 and Type 4 (NR juices). The endpoints which refer to the stomach and intestine are reported. Data are reported as dissolved% values ($M_{ion}/M_0 \times 100$) and measured by means of UF/ICP-OES (see 4.3.1.2 in the Experimental section). *$p \leq 0.05$, **$p \leq 0.01$, ***$p \leq 0.001$ and ****$p \leq 0.0001$ compared to the corresponding juice 1 timepoint. (B) Dissolution of NM110 (50 mg L^{-1}) upon the application of the cascade *in vitro* digestion assay in the Type 1 formulation with decreased concentrations of enzymes (overall enzyme content) (100, 70, 50, 25 and 0%; the latter corresponds to the Type 3 formulation graph in panel A). The endpoints which refer to the stomach and intestine are reported. Data are expressed as mean ± standard deviation (*n* tests = 3). Data are reported as dissolved% values ($M_{ion}/M_0 \times 100$) and measured by means of UF/ICP-OES (see 4.3.1.2 in the Experimental section). *$p \leq 0.05$, **$p \leq 0.01$, ***$p \leq 0.001$ and ****$p \leq 0.0001$ compared to the corresponding juice 1 timepoint.

© 2024 The Author(s). Published by the Royal Society of Chemistry

Open Access Article. Published on 08 December 2023. Downloaded on 2/2/2024 12:01:41 PM. This article is licensed under a Creative Commons Attribution-NonCommercial 3.0 Unported Licence.

Interestingly, specific ion sequestration triggers dissolution and cooperates with the acidic pH of the stomach to promote further dissolution. This cooperative mechanism of action is clearly demonstrated in the stomach compartment where the acidic pH remains the main force in driving ZnO particle dissolution, independently from the juice types (Fig. 2A). However, when digestion of NM110 is performed under conditions of acidic pH only (Fig. 2A, Type 4), the dissolution corresponds to *ca.* 60%, whereas in the presence of digestive enzymes and acidic pH the dissolution is pushed to almost 100%. Notably, the reduction of dissolution by the complete absence of the enzymatic component leads to a down estimation of dissolution of metal containing nanoparticles in the case of use of simplified simulant juices. When prediction of biodurability is the scope of the work, the use of simplified juice formulations may attribute false interpretations to the conclusions drawn. The presented results highlight, for the first time, and reinforce the importance of using physiologically relevant conditions (which must be extrapolated by the exposure scenario of interest) to assess NF biodurability for hazard assessment. In particular, based on the data presented above, the Type 1 formulation is a preferable option for metal containing NFs for which the interactions of soluble ions with known biomolecules (such as enzymes) are verifiable.

Notably, the dissolution parameter informs the user about biotransformation of digested NFs and whether they are still available at nanoscale dimensions upon digestion. The identification of NFs of different sizes or soluble ions upon intestinal digestion can allow them to be related to potential toxicity (either local or systemic). Moreover, in case of gradual dissolving NFs, the co-existence of digested NFs and the respective released soluble molecular ionic species may be responsible for toxicity.[2] Under such conditions, we argue that in addition to dissolution measurements, the metal ion speciation in a relevant exposure scenario (*e.g.*, using complete digestive formulations) by means of chemical equilibrium tools, can provide further information leading to a clearer hazard assessment.

2.3 Robustness of ZnO findings using standardised simulant OGI juices in Type 1 and Type 3 formulations (DIN/ISO 19738)

In order to demonstrate the ability to use dissolution% (or half-life) in OGI fluids as a grouping criterion, we explored the dynamic range of the assay using a quickly dissolving material (represented by NM110), gradual dissolving NFs (represented by SiO_2 NM200 and $BaSO_4$ NM220), and very slow dissolving NFs (represented by TiO_2 E171).[2] The cascade *in vitro* dissolution assay was carried out with the DIN/ISO 19738 standard juices (referred to as DIN from now on), which are almost identical to the NR juices, but simpler (as highlighted in Table S1†). For all four materials (ZnO, SiO_2, $BaSO_4$, and TiO_2), we applied the Type 1 formulation (DIN) and Type 3 formulation (DIN) (Scheme 1), motivated by the potential simplification of the method for grouping purposes, where enzyme-free Type 3 juices enable automated dissolution testing with much reduced manual handling. Although Type 3 and 4 NR impacted dissolution quite similarly (Fig. 2A), for studies by means of DIN standard juices, we preferred Type 3 to Type 4, because, the first includes the organic portion (*e.g.* mucin, uric acid, and urea, see Table S3†), which although not having a clear impact on dissolution (Type 1 *vs.* Type 2 in Fig. 2A), are known as stabilizers of colloidal suspensions (contrarily to acidic solutions of inorganic salts as in the case of the Type 4 formulation) (see Table S3†).[8]

2.3.1 Benchmark quick dissolution NM110. With an initial concentration of NM110 in saliva (67 mg L^{-1} in the DIN juice that is quite comparable to the 50 mg L^{-1} reported above for the NR juice), the enhancing effect on dissolution of the intestinal enzymes was reproduced in the DIN juice (Table S5†): the Zn concentration dropped from 68% dissolved (Type 1 formulation, DIN) to 0.36% dissolved (Type 3 formulation, DIN) when the enzymes were omitted. However, no such effect was observed in the stomach phase, where the measured Zn concentration remained high at 78% dissolved (DIN Type 1) and 99% dissolved (DIN Type 3). This is in accordance with data shown for Type 1 and 3 NR formulations in the stomach phase where no statistical significant differences were visible (Fig. 2A, st). Here for the DIN based formulations, we observed even an apparent reduction of dissolved% in the presence of enzymes (DIN Type 1 juices); we investigated the phenomenon more in depth by testing different methods of separation (particles from dissolved ions) and of quantification (type of calibration and optional microwave digestion). In short, separation of the stomach sample by 1 h ultracentrifugation at 40 000×*g* (Table S5†) tended to reduce the measurable ion content as compared to separation by 0.02 μm filtration (the latter is not indicated with * in Table S5†). In DIN Type 1 intestinal juice however, regardless of the separation method, the quantification method specifically had a high impact on the dissolved content that varied between 17% and 68%. We attribute the losses during separation and quantification to the scavenging of ions by enzymes. In support of this explanation, the destruction of the enzymes by microwave digestion resulted in the highest measured dissolved content (Table S5,† ** row).

For either the separation or the quantification method, the dissolved content in DIN Type 3 intestinal juice remained at or below 1% (see also next Fig. 4). Using the ultrafiltration method, the kinetics of NM110 dissolution with additional sampling time points (Fig. S6†) showed a very quick dissolution as expected: at 5 minutes, the stomach juice was added to the saliva juice, and already the first sampling at 10 minutes indicated full dissolution, *i.e.* a half-time of much less than 10 minutes. The tests in the DIN Type 3 medium were not performed in triplicate but showed less than 3% scatter between the different samplings in the stomach phase, which all range between 95% and 100% dissolved content (Fig. S6†). This evidence is in accordance with the data already reported in Fig. 2A with NR juices, demonstrating once again the main role of the acidic pH in promoting Zn dissolution in the stomach compartment.

Comparing the dissolution results of the two Type 3 formulations implemented (NR and DIN, Fig. 2A and S6†) we found comparable results, that is a drop in the dissolution efficiency at the intestine site, when the Type 3 formulation is implemented.

© 2024 The Author(s). Published by the Royal Society of Chemistry

Open Access Article. Published on 08 December 2023. Downloaded on 2/2/2024 12:01:41 PM.
This article is licensed under a Creative Commons Attribution-NonCommercial 3.0 Unported Licence.

Such a drop was more pronounced when the Type 3 DIN formulation was applied. This is tentatively attributed to the absence of BSA in the DIN juices that, although it does not have a fundamental role in promoting NM110 dissolution (NR Type 2 where BSA lacks shows comparable results of NR Type 1 formulation, Fig. 2A), can stabilize the Zn^{2+} ions against flocculation and re-precipitation to form new particles upon the increase in pH under neutral conditions in the intestine compartment.[40]

2.3.2 Benchmark gradual dissolution SiO_2 NM200 and $BaSO_4$ NM220. SiO_2 NM200 and $BaSO_4$ NM220 have both been considered as "partially soluble" in the case of pulmonary dissolution[42] and they represent opposite cases of pH-dependence: $BaSO_4$ is practically insoluble at neutral pH, but undergoes dissolution under lysosomal (pH4.5) conditions. SiO_2 in contrast is more stable at acidic pH than at neutral or basic pH. We observed that $BaSO_4$ NM220 dissolution is not only governed by pH, but especially in the intestine phase the enzymes shift the dissolution from 11% to 28% (Fig. 3A). For SiO_2 NM200, the ion concentration within DIN Type 1 was higher than that of the enzyme-free DIN Type 3 to a certain extent, but to a lower level than for $BaSO_4$ (Fig. 3B). All of the resulting dissolved percentages remain far below the daily uptake of SiO_2 NM as proposed by EFSA cutoffs,[43] and so we can speculate that the enzymes are not critical to the assessment of this material.

2.3.3 Benchmark very slow dissolution TiO_2 E171. The dissolution and transformation behavior of TiO_2 E171 was also assessed in both Type 1 and Type 3 formulations (DIN juices) (Fig. 3C). Within the TEM comparison of TiO_2 E171 (Fig. S7†) with and without enzymes, no significant difference can be observed in the digestive intestinal compartment. Furthermore, this was confirmed through selected area electron diffraction (data not shown). TiO_2 NM105 which was used as another benchmark material behaved similarly and thus showed no significant transformation after the cascaded treatment. The biopersistence in both media was also confirmed through XRD evaluation (Fig. S7†). Here the data showed no new peaks and no significant change in peak width. Remarkably, however, the interaction of enzymes with the particles (DIN Type 1) increased the ion concentration compared with the enzyme free intestinal fluid (DIN Type 3). This detectable increase in Ti-ion concentration occurred to a very low level of <0.05% and was observed for both TiO_2 materials, E171 and NM105 (Fig. 3C). This is explicable through the complexation of ions with the enzymes, shifting the dissolution kinetics as that for ZnO NFs.

2.4 Application of the cascade *in vitro* digestion assay to 16 materials to enable a similarity assessment for grouping purposes

We applied the cascaded *in vitro* dissolution assay to many more substances, both as NFs and as non NFs. We used Type 3 (DIN) formulations with simplified OGI juices (Table S3†). We selected Type 3 (DIN) and not the other formulations motivated by the potential simplification that this formulation can provide, thus favoring a potential automation of the digestion assay with much reduced manual handling. Across all case studies and across the three OGI compartments, the obtained dissolved concentration (see next the data presented in detail) spans six orders of magnitude from 20 mg L^{-1} (fully dissolved ZnO in stomach), down to 0.02 μg L^{-1} (DPP pigment in stomach). In the following section, we present and discuss case studies in order of decreasing dissolution.

2.4.1 Screening of dissolution kinetics and transformation by using the Type 3 formulation (DIN)

2.4.1.1 ZnO NFs and non-NFs. The dissolved percentage of the three ZnO forms (NF, NM110; coated NF, NM111; non-NF, NM113) in Type 3 DIN, were strikingly similar in all three cascaded compartments (Fig. 4). All ZnO materials remained undissolved in saliva, and then dissolved more than 90% within 5 minutes in the stomach simulant (Fig. S6†). Immediately after switching to the intestinal simulant, the free Zn ions were decreased to less than 20% of the total Zn content, and within 30 minutes (corresponding to the experimental point referred to as Int 1 thoroughly the manuscript), less than 1% remained as free Zn ions. This behavior represents the limited solubility of Zn ions at the near-neutral pH of the intestinal fluid in the absence of enzymes. However, this effect was reduced in the case of Type 3 NR (*ca.* 40% at Int 1) where the presence of albumin may act as an ion stabilizer; hence the fraction of bioavailable ions remained

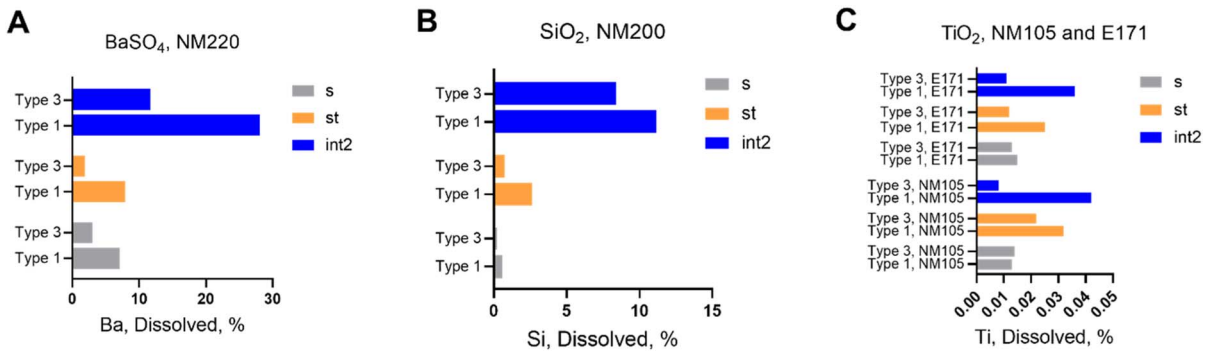

Fig. 3 Dissolution of (A) $BaSO_4$ NM220 (394 mg L^{-1} initial element concentration in saliva), (B) SiO_2 NM200 (313 mg L^{-1}), and (C) TiO_2 NM105 and E171 (400 mg L^{-1}), upon the application of the cascade *in vitro* digestion assay in Type 1 and Type 3 (DIN). Dissolved% was measured by filtration/ICP-MS (see 4.3.2.1 in the Experimental section). This dataset is $n = 1$.

Open Access Article. Published on 08 December 2023. Downloaded on 2/2/2024 12:01:41 PM.
This article is licensed under a Creative Commons Attribution-NonCommercial 3.0 Unported Licence.

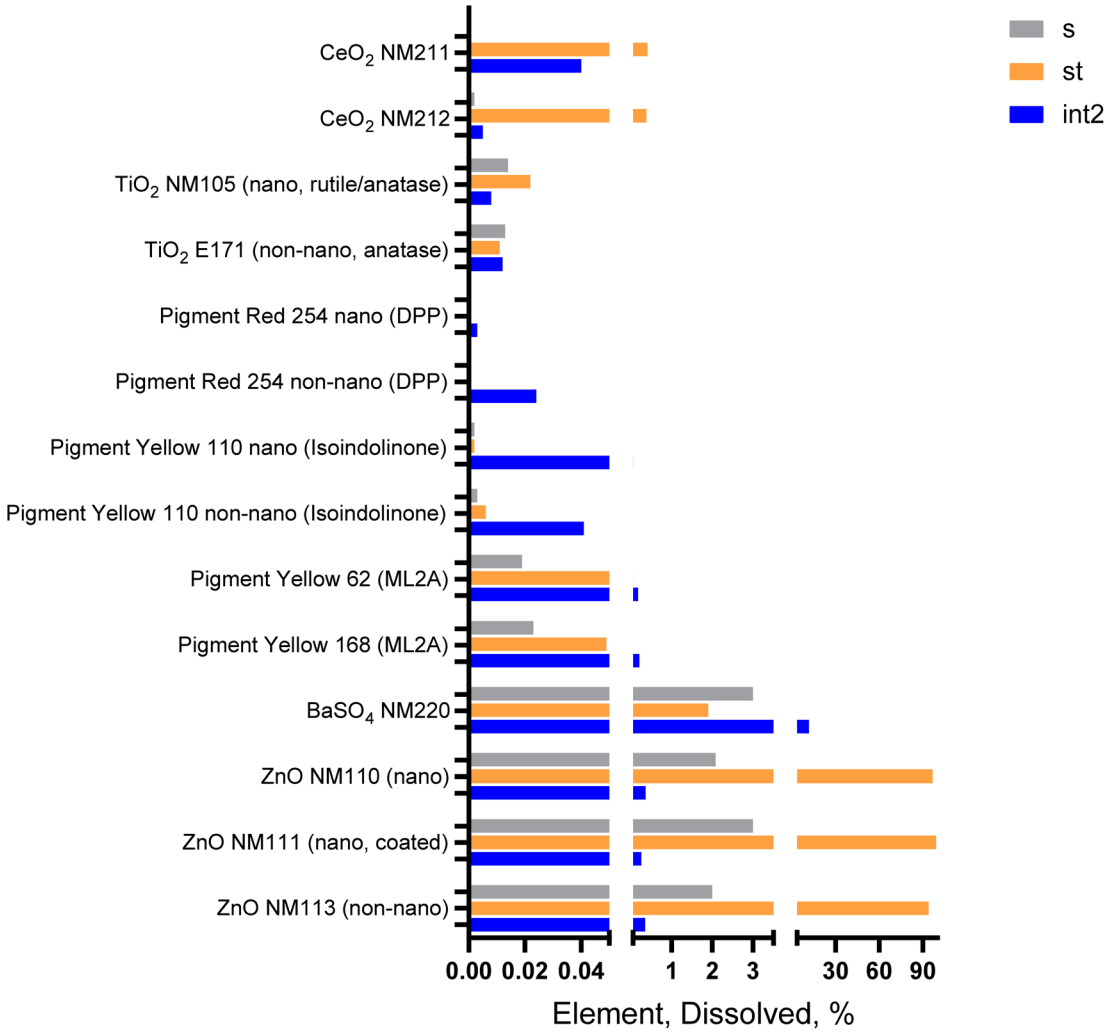

Fig. 4 Application of the cascade *in vitro* digestion assay with the Type 3 formulation (DIN juice) for grouping purposes: Dissolved concentration in each of the three compartments: saliva (blue bars), stomach (orange bars), intestine (grey bars). Numerical values of the measured concentrations and the respective % dissolved fraction are given in Table S5† (dissolved% was measured by filtration/ICP-MS for the inorganics and by filtration/UV-vis for the organics, see 4.3.2.1 in the experimental section).

more soluble in the intestinal environment. However, despite the difference between the Type 3 formulations (NR *vs.* DIN), the dissolution measurement by using the Type 3 formulation (DIN juices) did not affect the detection of NFs in the first 30 minutes of intestinal digestion (where all juices disappear quite completely); hence, an acceptable juice formulation can be retained to fulfill the EFSA guidance[4] for which no nano-specific assessment is required if the complete dissolution of a NF is demonstrated in the first 30 minutes of intestinal digestion.

2.4.1.2 CeO_2 NFs. Both NFs of CeO_2 showed very low dissolution below 1%, with values comparable to the TiO_2 benchmark of an insoluble material (Fig. 4 and Table S5†). For both CeO_2, NM212 and NM211, spICPMS (data not shown) identified similar trends: low agglomeration in the saliva and intestine, but higher agglomeration in the gastric juice. This phenomenon seems to be dictated by the substance primarily, and is not explicable by pH changes, especially not after the dilution required for spICPMS measurement.

2.4.1.3 Organic pigment NFs and non-NFs. Three different pigment classes were investigated and showed that organic pigments were as insoluble as TiO_2 or CeO_2, with the exception of metal-lake pigments, which showed very slow dissolution (Fig. 4).

The isoindolinone substances have a dissolved concentration in the stomach comparable to that of TiO_2 or CeO_2 NFs and non-nanoforms, whereas in the intestine the dissolution was about 5-fold more than that in the stomach. There was no significant difference between the NFs and non-NFs. The analysis of crystallinity (Fig. S8†) confirmed that the pigment remained unchanged after incubation with the OGI digestive fluids.

The NFs of metal-lake pigments (ML2A class) were comparable to that of SiO_2 with respect to dissolved concentration: 20-to-50-fold higher than that of TiO_2, 20-to-50-fold lower than that of ZnO. Furthermore, the crystallinity analysis shows signs of transformation with shifted peaks (Fig. S8†). The substance

© 2024 The Author(s). Published by the Royal Society of Chemistry

Open Access Article. Published on 08 December 2023. Downloaded on 2/2/2024 12:01:41 PM. This article is licensed under a Creative Commons Attribution-NonCommercial 3.0 Unported Licence.

classes of lake (metal-precipitated) pigments were previously found to dissociate under physiological conditions.[44]

The DPP substance appeared insoluble in stomach and intestine compartments. It had 100-fold lower dissolved concentration than TiO_2, but the dissolved percentage in the intestine was in the order of the dissolved percentage of TiO_2 in the same fluid. At an extremely low level, the highest measurable dissolved content of maximum 0.024%, with 0.143 mg L^{-1} dissolved concentration is found in the intestine simulant with bile salts and a nearly neutral pH of 6.5. Also in this case, there is no significant difference between the NF and non-nano-form.

The observed lack of bioavailability of purely organic pigments is in accordance with *in vivo* findings of oral gavage experiments and the current Registration, Evaluation, Authorisation and Restriction of Chemicals (REACH) data,[45,46] and sets them apart from gradually dissolving metals and metal oxides.[23,47,48] The metal-laked pigments might therefore require a separate assessment. One notes that the analysis of abiotic reactivity, abiotic pulmonary dissolution, *in vitro* reactivity and *in vivo* inhalation also suggested the non-grouping of metal-laked pigments.[49,50]

2.4.2 Towards grouping: similarity of dissolution behavior exemplified by the assessment of Type 3 DIN and Type 1 NR data, each analyzed by two different similarity algorithms. For the purpose of grouping NFs with respect to toxicity following oral exposure, the acquisition of comparative data on OGI dissolution is required.[2] The GRACIOUS grouping framework[11] provides the option to conduct a quantitative similarity assessment of the data obtained by the application of similarity algorithms. Here, by applying two different algorithms (x-fold or Bayes factor algorithms), we evaluated the similarity within two homogenous datasets obtained using the same analytical method (the cascade *in vitro* assay) but two different juice formulations (Type 1 NR and Type 3 DIN); the datasets refer to the % of dissolution (at the end of each stomach or intestinal cascaded phase) (Fig. 5 and S9†). In particular, we aim to explore how robust the conclusions on NF similarity are, when different algorithms are applied to the same raw data or when the same algorithm assesses different OGI dissolution data sets. The similarity plots display materials in identical order and can thus be directly compared (Fig. 5 and S9†).[51] The pairwise comparison is shown as a color-coded similarity distance of the dissolution data obtained in stomach phases of both Type 3 DIN juice (Fig. 5a and b) (or in the intestine phase Fig. S9a and b†) and Type 1 NR juice (Fig. 5c and d, S9c and d† in the intestine phase). Red represents high similarity and blue colour represents low similarity, but the numerical values of the colour code are specific to each distance metric (algorithm), as explained by Jeliazkova *et al.*[51] The benchmark materials TiO_2, SiO_2 and ZnO span the biologically relevant range from very slow to intermediate (gradual) to quick (complete) dissolution (during the OGI passage). Accordingly, the benchmark pairwise comparison of TiO_2 *vs.* ZnO in the DIN dataset is yellow for low similarity in both algorithms (Fig. 5a and b). However, the bluish shade of pigment Red 254 (DPP) indicates that this material is an extreme case with te slowest dissolution, slower than the benchmark TiO_2. Similarity distances do not show the ranking (Fig. 5), where pigment Red 254 stands out as having the lowest solubility, lower than that of TiO_2. Only one pairwise comparison shows high similarity of pigment Red 254, namely the comparison of NFs and non-NFs. Analogously, both algorithms identify the high similarity of both NFs of CeO_2 (NM211 and NM212), of the two metal-lake pigments Yellow 62 and Yellow 168, as well as of all NFs and non-NFs of ZnO (Fig. 5a and b). Jeliazkova *et al.*[51] found that the x-fold algorithm and Bayes factor algorithm were mutually consistent, with differences especially in the assessment of the most similar pairs of NFs. This is confirmed here. Indeed, in Fig. 5, (a *vs.* b) and (c *vs.* d) indicate that the same pairs of NFs are highly similar (red colors), *e.g.*, the pairs of pigments in NFs and in non-NFs, or the pairs of different ZnO NFs. They also indicate the same pairs of NFs to be very different (blue colors), *e.g.* the TiO_2 E171 or the pigment Red 254 compared to any other material, because these are the least-dissolving materials (Fig. 5a and b). The pigments were only tested in DIN Type 3 juices, but for the other cases highlighted above, the finding is confirmed in the NR Type 1 juices, in both algorithms (Fig. 5c and d). The similarity analysis of the intestine phase is presented in Fig. S9†: for both DIN Type 3 fluid and NR Type 1 fluid, the insoluble materials (all NFs and non-NFs of TiO_2, all NFs of CeO_2, and NFs and non-NFs of pigment Red 254 and Yellow 110) stand out in bluish shades against the partially soluble materials (all NFs of SiO_2 and both metal-lake pigments Yellow 62 and Yellow 168). As discussed above, the tendency of ZnO to reprecipitate is different between the fluids, but in both fluids, and both algorithms, the mutual similarity of ZnO NFs is confirmed. Differences between the x-fold and Bayesian algorithms appear especially in the assessment of the most similar pairs of NFs. We argue that although the absolute level of dissolution may be modulated by element-specific interaction with enzymes (Fig. 4 and 5), the comparison of same-substance NFs as required for grouping shows a robust result for both DIN and NR juices, both Type 1 (more realistic) and Type 3 (easier to handle). We also suggest the cropping of the data matrix to the biologically relevant range (here: 0.01% dissolved, from TiO_2 E171), as implemented in the GRACIOUS e-tool blueprint[29] and demonstrated for pigment inhalation similarity.[50] Cropping even lower values would remove the apparent uniqueness of the pigment Red 254, and instead would focus the assessment on the cases of gradual dissolution. This would further increase the consistency, since the general shift towards more reddish colors (higher similarity) with the DIN fluid is distorted by the very dissimilar outlier of pigment Red 254 with its extremely low solubility. Finally, for drawing conclusions on the similarity between NFs, combining information on dissolution with other key physicochemical, toxicokinetic and/or hazard data will be needed.[51]

3 Discussion

The importance of using dissolution testing to predict the biodurability of NMs is well established. Physiologically significant simulating juices are claimed to be predictive, although little comparison between *in vitro* and *in vivo* dissolution has been performed due to technical difficulties in assessing the

Open Access Article. Published on 08 December 2023. Downloaded on 2/2/2024 12:01:41 PM.
This article is licensed under a Creative Commons Attribution-NonCommercial 3.0 Unported Licence.

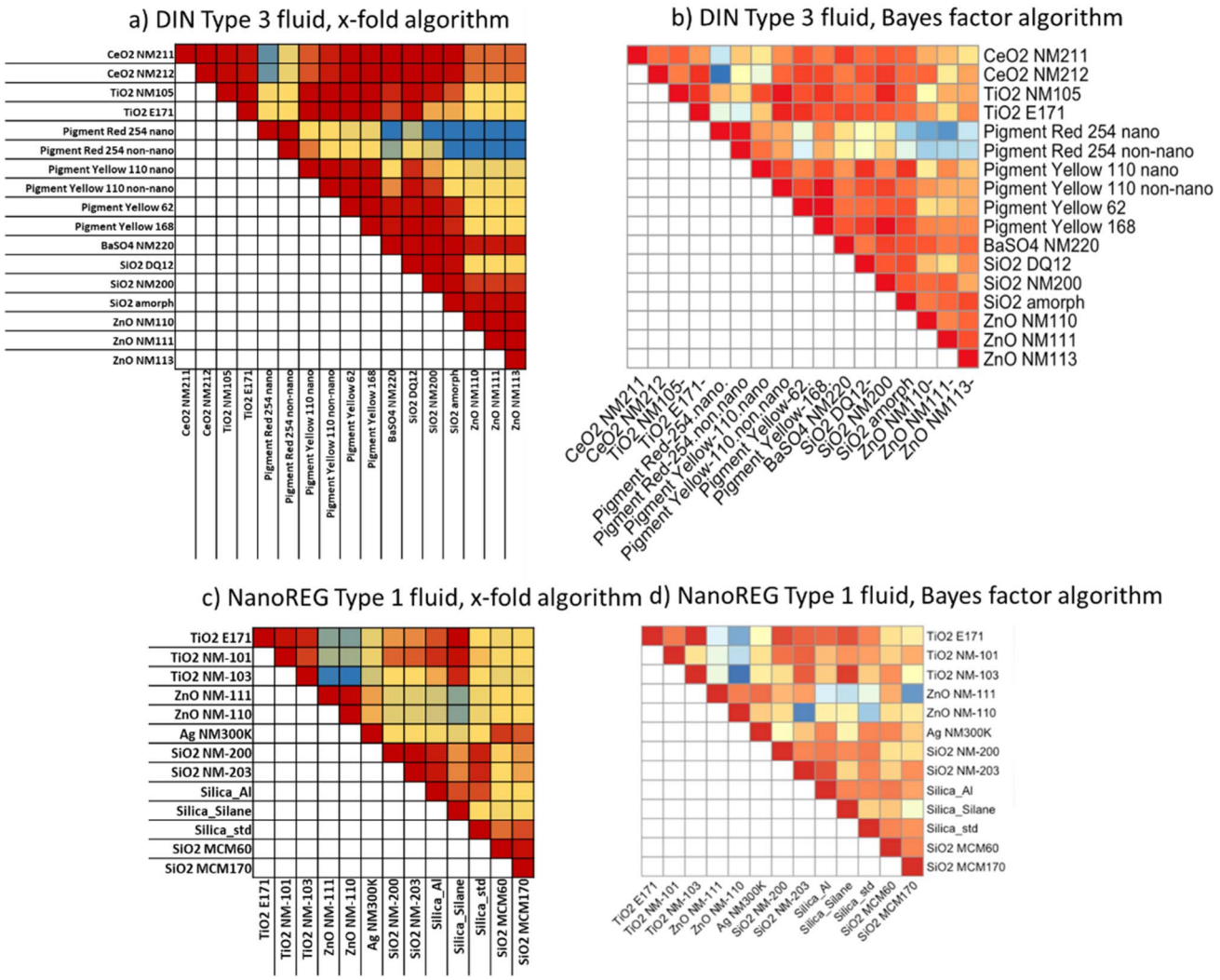

Fig. 5 Similarity assessment of dissolution of case studies and benchmark materials assessed *via* the cascade incubation method. The identical data of % dissolved in the stomach juice are represented by two different similarity algorithms, namely (a and c) by the x-fold algorithm; (b and d) by the Bayes factor algorithm. See Fig. S9† for analogous evaluations of the intestine phases. Juices without enzymes (a and b are DIN Type 3 juices with the numerical values in Table S5† and Fig. 4) or with enzymes (c and d are NanoREG Type 1 juices with numerical values in Table S7†). Color codes were adjusted to each dataset with red indicating similarity, and blue indicating difference: X-fold: Type 3 DIN: red = 1, yellow = 50, and blue = 500 000; Type 1 NanoREG: red = 1, yellow = 5, and blue = 250. Bayes: Type 3 DIN: red = +2, yellow = −8, and blue = −22; Type 1 NanoREG: red = +2.5, yellow = −1, and blue = −4.5.

dissolution behavior *in vivo*. The need for using enzymes or other biomacromolecules is widely debated; however, little analytical evidence is currently available demonstrating their effective impact on the degree of dissolution and biotransformation in the OGI tract. In this study, by applying the cascade *in vitro* digestion assay, we provided a systematic analysis and quantitative evidence that digestive enzymes impact the dissolution and biotransformation of NFs and non-NFs. To do this, we employed a multitude of analytical techniques for post dissolution characterization (UF, ICP-AES, TEM, SAED-EDX, FFF, spICPMS, and XRD) which allowed a detailed understanding of the underlying mechanism by which enzymes act as ion scavengers (in some cases also in conjunction with physiological pH), thereby increasing the dissolution kinetics of the dissolving NFs. This is regarded as a real biological effect that impacts biotransformation of NFs in digestive juices by means of the modulation of 'bio-accessible soluble molecular species, *i.e.*, soluble species available for intestinal adsorption. Noteworthily, the dilution occurring during the cascaded addition of the simulant digestive juices can also contribute to augment the dissolution: a material with a solubility limit below the final concentration, and no sensitivity to the different juices, would remain at the same absolute ion concentration, but the "%-dissolved" value would increase two-fold from saliva to the stomach and again two-fold from the stomach to intestine juices. However, our data show that the absolute ion concentrations do not remain constant for any of the materials. Instead, each material has its own specific sensitivity to different juices (see Tables S4, S5 and S7†).

© 2024 The Author(s). Published by the Royal Society of Chemistry

Open Access Article. Published on 08 December 2023. Downloaded on 2/2/2024 12:01:41 PM.
This article is licensed under a Creative Commons Attribution-NonCommercial 3.0 Unported Licence.

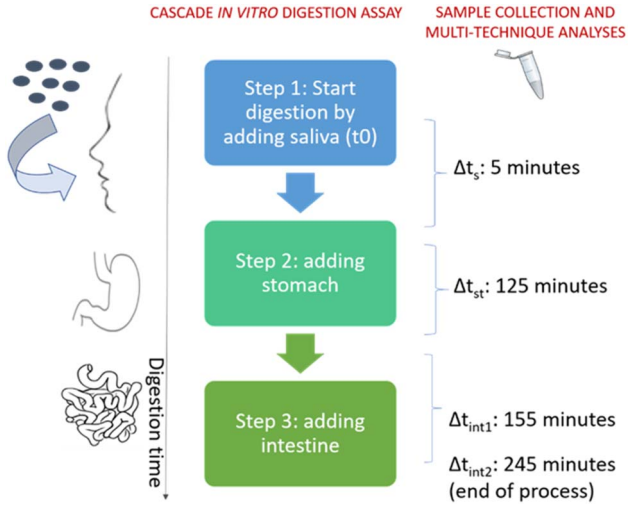

Scheme 2 Schematic representation of the 'cascade *in vitro* digestion assay'. The scheme describes the consecutive addition of the simulant digestive juices over a total of digestion time of 245 minutes. The samples were collected at different elapsed times of incubation. The Δt refers to the time interval occurring between t_0 and the sampling times, which are 5, 125, 155 and 245 minutes, respectively. Post-digestion analysis is based on a multi-analytical technique approach that varies depending on the studied NF.

The enzyme mediated ion scavenging mechanism can be appreciated when NFs of different materials (*e.g.*, ZnO, TiO_2, SiO_2, and BaSO4) are digested by different types of juice simulants (Type 1 formulation, NR or DIN/ISO 19738). The reported results are in line with recent findings showing a similar mechanism albeit exerted by histidine on the dissolution of ZnO NPs in artificial sweat juices.[13] The enzyme mediated dissolution enhancement is a phenomenon not universally appliable for all substances, but can be highly relevant in the case of strong affinity of enzymes to the released ions. This effect is similarly observed with different organic acids that are employed to simulate lysosomal conditions (incl. enzymes).[52–54] However, while the enzymes can clearly enhance NF dissolution, negligible effects are observed on particle size transformation with little influence on particle agglomeration.

Based on these observations, herein, we provide a rational design of analytical criteria for dissolution testing: when predictive precision is needed (where the assessment of bioavailable soluble molecular species is needed to link their impact on toxicity *e.g.*, *in vitro*/*in vivo*), juices with high physiological relevance are strongly recommended. Therefore, we recognize "complete" juices (inorganics + enzymes + other organics, Type 1 formulation) as the preferable option in dissolution tests. We also stress the importance and the use of 'complete juice' for mechanistic studies on substances of gradual dissolution,[12,55] where the chemical nature of the released ion is well known to be toxic (*i.e.* copper ion). However, for comparison of different forms of a substance, a rapid and efficient screening comparison between different target NFs and a known NF (the source material) with respect to a functional property (*i.e.*, dissolution in the OGI) is increasingly required, or, more generally, a comparison of many different nanoforms and non-NFs.[2,6] In such cases, easy-to-handle and robust methodologies and simplified juices (with less practical issues in sampling and homogeneity) can be beneficial such as the Type 3 formulation (inorganics, other organics, and w/o enzymes). Furthermore, in the case of gradual or slow dissolving NFs, the simplified juices systematically tended to exhibit less dissolution than complex juices, offering a conservative assessment with regard to the regulatory criterion for the need to perform nano-specific risk assessment according to EFSA guidance.[4] Hence, the outcomes by using Type 3 formulations are relevant even for regulatory needs. Finally, by applying two different similarity algorithms on homogeneous data matrices (*i.e.*, produced by the same cascade method but different juice formulations, Type 1 or 3), we demonstrated robust conclusions of similarities among 16 materials (both NFs and non NFs) allowing a clear classification of some tested NFs as quick, gradual and very slow dissolving (according to the recent definitions provided in Di Cristo *et al.*).[2] We argue that although the absolute level of dissolution may be modulated by element-specific interaction with enzymes (Fig. 4 and 5), the comparison of same-substance NFs as required for grouping is a robust result for both DIN/ISO 19738 and NR juices, both Type 1 (more realistic) and Type 3 (easier to handle) formulations.

4 Conclusions

The data presented in the study demonstrated the importance of rational design of analytical criteria for dissolution testing. The reported data referring to a range of metal and non-metal containing NFs and non NFs indicate the formulations (reported as Type 1 formulations, which include "complete" juices, *i.e.,* inorganics + enzymes + other organics) as the preferable option when mechanistic studies as well as hazard assessment are needed for substances; when, indeed, a comparison of many different nanoforms and non-NFs is needed for grouping purposes, we recommend the use of simplified and easy to handle formulations (*e.g.* Type 3 or 4 where enzymatic or organic components are reduced or absent). In this regard, the presented data demonstrated the feasibility of using dissolution as a parameter in similarity approaches for diverse materials. Here, we recommended the selection of the biologically relevant concentration range in order to obtain physiological significance in the similarity distances given by the algorithms (*e.g.*, by cropping the data matrix at very low dissolution). The combined learnings also provide guidance for future automation of NM testing, as desired for grouping by high throughput screening. For any of the formulations discussed in the work, standard or other common known juices (*e.g.* DIN, NR or FaSSIF/FaSSGF) can be implemented.

4.1 Experimental

All chemicals and reagents used were obtained from Merck Millipore (Milan, Italy), unless otherwise stated.

4.2 Nanomaterials and case studies

ZnO NFs (NM110, NM111), ZnO non nano (NM113), SiO_2 NFs (NM200), TiO_2 NFs (NM105), $BaSO_4$ NFs (NM220) and CeO_2

Open Access Article. Published on 08 December 2023. Downloaded on 2/2/2024 12:01:41 PM. This article is licensed under a Creative Commons Attribution-NonCommercial 3.0 Unported Licence.

NFs (NM211 and NM212) were obtained from the JRC Nanomaterials Repository (Ispra, Varese, Italy). Food grade non-nano TiO_2, E171, was obtained from Venator (Germany). A total of 6 commercialized organic pigments, sorted into 3 chemical classes (ML2A, Isoindolinone and DPP), were obtained from BASF SE, and were described elsewhere.[49,50] These materials were used within the scope of the H2020 project "GRACIOUS: Grouping, Read-Across, CharacterIsation and classificatiOn framework for regUlatory risk assessment of manufactured nanomaterials and Safer design of nano-enabled products".

4.3 Cascade *in vitro* digestion assay

The *in vitro* setup consisted of a cascade addition of simulant juices (representing the saliva, stomach, and intestine) to a NF suspension, which has been described in several publications.[8,18–20,22] This assay was performed independently by two laboratories employing the Type 1 formulation (see below) of two different juice compositions (NaNoREG, 'NR juice' or 'DIN 19738 juice') and relative sub-groups, Type 2, 3 and 4 (refer to Table S1–S3† for each molecular juice composition).

4.3.1 Cascade *in vitro* digestion assay employing the Type 1 formulation (using NR juices)

4.3.1.1 Sample sonication and preparation of juice formulations. In order to simulate the digestion process, a modified version of the *in vitro* dissolution test described by our recent work was followed.[2,12,18–20] Here, the overall volume of the process was scaled down three-fold to increase its practicality. NM110 was dispersed in MilliQ water at a concentration of 2.56 mg mL^{-1}, The suspension was sonicated using a Bandelin Sonopuls Ultrasonic Homogenizers HD 2200, equipped with a 3 mm probe (BANDELIN electronic GmbH & Co. KG; Berlin, Germany). An amplitude of about 30% of the maximum (302 μm) was applied for 5 minutes to gently favor nanoparticle dispersion in the suspension. Before dilution, the stock suspension was left to equilibrate at room temperature for 30 minutes. The suspension was then diluted in MilliQ water at working concentrations, from 25 to 1000 mg L^{-1}. Juices representing the saliva, stomach, duodenum and bile, but without proteins and enzymes, were prepared the day before the experiments and incubated overnight at 4 °C. The following day the completed juices (with proteins and enzymes) were heated to 37 °C for 2 h before use. To begin, 0.3 mL of NM110 in MilliQ water at different concentrations was transferred into a falcon tube. The digestion process started when 2 mL of saliva juice was added to the NF suspension (pH 6.8). After 5 minutes at 37 °C (shaking at 80 RPM), 4 mL of stomach juice was added and the falcon tube was then incubated for another 125 minutes at 37 °C (shaking at 80 RPM, pH of 2.5 ± 0.5 was set). At the end, 4 mL of duodenal fluid, 2 mL of bile salts and 0.6 mL of 84.7 g L^{-1} sodium bicarbonate were added (pH of 6.5 ± 0.5 was set). Intestine incubation (37 °C and shaking at 80 RPM) was stopped at two timepoints, after 155 and 245 minutes of digestion.

4.3.1.2 Cascade in vitro digestion assay. Scheme 2 outlines the applied cascade *in vitro* digestion assay. Passage of the dispersed NF through the OGI tract was simulated by the sequential addition of different volumes of simulant digestive juices (saliva, stomach and intestine). The assay simulates human oral digestion under fasting conditions accounting for pH 'jumps', transit times in the different digestive compartments, compartment volumes and changes in juices (both molecular composition and relative concentrations) typically undergone in humans in four hours of digestion in the absence of food.[25,56,57] Over the entire digestion process, we followed the biotransformation of NFs by collecting the samples at specific elapsed times in each subsequent simulant digestive juice. A multi-analytical technique approach (*i.e.*, ultrafiltration, UF or filtration, ICP-OES or ICP-MS, TEM, FFF and XRD) was applied to qualitatively or quantitatively depict the complexity of the biotransformation process including dissolution and, in specific cases, size and chemical characterization (see 2.3.1.3 below).

4.3.1.3 Post digestion analytical processing. Ultrafiltration (UF) and inductively coupled plasma-optical emission spectrometry (ICP-OES): ultrafiltration of digested samples was performed using Amicon Ultra 15 mL centrifugal 3K filters according to the manufacturer's instructions. The flowthrough containing free ions only was then processed by ICP-OES. The samples were dissolved in aqua regia (HCl–HNO3, ratio 3 : 1) at a final concentration of 10% v/v with MilliQ water and then analyzed by ICP-OES (Agilent 720/730 spectrometer). ICP calibration standards were used to construct a multipoint standard curve.

Transmission electron microscopy (TEM): the NFs incubated with the digestive juices were treated by two steps of centrifugation (21 230×*g*, 10 minutes, at 4 °C) and subsequently washed with MilliQ water, to remove organic matter and salts derived from simulant digestive juices. TEM samples were prepared by dropping 5 μL of water-diluted solution of NFs on carbon-coated copper grids (Carbon 150 Mesh Cu). Annular dark field scanning transmission electron microscopy (ADF-STEM) images were acquired by means of a JEM-1400Plus microscope (JEOL), with a LaB_6 thermoionic source, operated at 120 kV. The corresponding energy-dispersive X-ray spectroscopy (EDX) data were acquired on the same microscope using a JED-2300 detector from JEOL (silicon drift type, detector area 30 mm^2). Cu and C peaks are always present in the EDX spectra from these specimens, respectively, due to the TEM grid and to the carbon support film.

Field-flow fractionation (FFF): FFF analyses were carried out with an Agilent 1200 system (degasser, quaternary pump, autosampler, and DAD detector, Agilent Technology) and flows were managed by using a Wyatt Eclipse Dualtec module. The separation device employed was a hollow fiber, the miniaturized version of an asymmetrical channel, to perform a hollow fiber flow field flow fractionation (HF5) analysis. The separation mechanism is described in Marassi *et al.* 2018.[58] The separation channel was a PES membrane (Nadir) commercially available, 17 cm long and with 0.8 mm ID. The detector flow was set to 0.35 mL min^{-1} and the detection wavelength was set to 280 and 380 nm, corresponding to protein and NM110 absorption maxima. A conventional FFF method is composed of four steps:

 © 2024 The Author(s). Published by the Royal Society of Chemistry

Open Access Article. Published on 08 December 2023. Downloaded on 2/2/2024 12:01:41 PM.
This article is licensed under a Creative Commons Attribution-NonCommercial 3.0 Unported Licence.

focus, focus inject, elution and elution inject. These ensure that (1) The mobile flow stream is equilibrated, (2) The injected sample is focused in a narrow band at the beginning of the channel, while smaller components (<cutoff) are filtered away, (3) The sample is eluted and separated into components by the hydrodynamical force generated by the cross-flow, and (4) The inlet is rinsed and the equipment is ready for further analyses. A flow-injection analysis (FIA), instead, only envisions the use of the last two steps with a zero crossflow, avoiding sample washout and minimizing membrane interaction; an in-between mode, the focus-FIA, is a FIA that retains steps 1 and 2 and simulates washing out of particles in a non-equilibrium state.[59] Results in focus-FIA mode yielded to the complete loss of NM110 signals confirming that dynamic environments are able to dissolve particles and only FIA mode can portray the digestion cascade. In FIA, the sample can be characterized in its entirety by optical detectors. The digestion cascade analyses were first carried out using a protein/enzyme free compartment as the mobile phase, to mimic the environment (salinity and pH) and subsequently using water as the mobile phase. The results (peak intensity and differences and absorption profile of compartments) (data not shown) showed that water provided the most advantageous signal noise ratio and increased sensitivity while reducing carrier viscosity and offering better on-line and offline compatibility towards other techniques. Therefore, water was then chosen as a carrier for all subsequent analyses. A calibration curve was built injecting a fixed amount of NM110 recorded at 380 nm (from 1.25 to 30 μg mL^{-1}), graphed *versus* intensity and peak area (Fig. S5†). These amounts reach below and above the calculated NM110 mass injected during digestion studies. Following the digestion protocol, each compartment plus the NM110 sample was injected (100 μL) and compared to an equivalent injection of the compartment alone, recording absorption at 280 nm and 380 nm and a full spectrum (200–800 nm).

4.3.2 Cascade *in vitro* digestion assay employing the Type 1 formulation (using DIN juice). The NFs and non nanoforms (NM110, NM111, NM113, NM211, NM212, NM220, NM200, NM105, E171 and 6 organic pigments) were dispersed with a BRANSON Sonifier 450D at an amplitude of 30% for 16 minutes within an inverted cup-horn sonicator to deliver an energy output of 7.35 W. A 50 mL Nalgene® bottle was used to reduce inorganic impurities. For fluids with enzymes, the enzymes were added after the sonication process. The saliva dispersions were stirred for 5 min at a temperature of 37 °C. After removing 5 mL of the dispersion for ion and transformation analysis, 21 mL of gastric juice was added and set to pH 2.0. After two hours of stirring at 37 °C, the next 5 mL sample was drawn and analyzed, and 25 mL of intestinal fluid was added, and a pH of 6.4 was set. Again, after two hours of stirring, the last sample was drawn and analyzed. Immediately after collection the drawn samples were split for analysis of dissolved components and of the remaining particles.

4.3.2.1 Post analytical processing. Filtration and inductively coupled plasma mass spectrometry (ICP-MS): for dissolution analysis, the dispersion was filtered through a 0.02 μm Al–Si syringe filter to remove particles and stop them from further dissolution. The filtrate was diluted with 0.1 n HNO_3 and was analyzed by ICPMS (PerkinElmer, Nexion 2000b). The dilution factor was adjusted so that the final analyte concentration was within the calibration range. The LOQ was calculated considering the 10σ-criterion and only values above the LOQ were taken into account.

Filtration and UV-vis analysis: for organic substances of the organic pigments, the dispersion was filtered through a 0.02 μm Al–Si syringe filter to remove particles and stop them from further dissolution. The filtrate was measured by using a Cary 5000 spectrometer with a detection limit of 0.001. The absorption was converted to concentrations by using the independently determined extinction coefficients of the same substances dissolved in concentrated acids.

X-ray diffraction analysis (XRD): for benchmark materials and organic pigments (which are crystalline), the sample was dried, spread on glass and subjected to XRD analysis of the crystalline identity (by using the characteristic diffraction peaks) and analysis of the crystallite size (by fitting the broadening of the peaks *via* EVA). The instrument D8 Advance Series 2 employed a Cu-Anode with 0.1° collimation; the diffracted X-rays were selected at 8 mm with a Ni 0.5 mm aperture (Soller 4°; Lynx-Eye 3°).

4.4 Dissolution calculation

Dissolution was calculated as % of dissolution according to the following equation:

$$\%\ \text{dissolution} = \frac{M_{\text{ion}}(t)}{M_0} \times\ 100 \tag{1}$$

where $M_{\text{ion}}(t)$ is the total ion concentration dissolved at time t and M_0 is the total ion content of the NF at time 0, supposing 100% dissolution (diluted according to the relevant compartment dilution factor).

Dissolution was also calculated as the dissolution rate at the correspondent digestion time (t) following the calculation described in several publications[42,60–62] and consistent with the first-order dissolution kinetics of ISO 19057:2017. In brief, the total ion mass dissolved at time t [$M_{\text{ion}}(t)$] as calculated in saliva (after 5 minutes), in the stomach (after 125 minutes) and in the intestine (after 155 and 245 minutes) was used to derive the dissolution k rate in each corresponding digestive compartment, as follows:

$$K_{\text{dis}} = \frac{M_{\text{ion}}(t)}{\text{SA}\ (t)} \Big/ \Delta t \tag{2}$$

where Δt is the sampling interval time over the entire digestive process (0–5, 0–125, 0–155 and 0–245 minutes) and SA (t) is the specific surface area at time t that is approximated as:

$$\text{SA}(t) = \text{BET}(t_0) \times (M_0 - M_{\text{ion}}(t)) \tag{3}$$

SA is obtained by multiplying the Brunauer–Emmett–Teller (BET) value at time 0 (t_0) with the $M_0 - M_{\text{ion}}(t)$. By using eqn (3), the conventional expression unit of k is ng cm^{-2} h^{-1}.

The dissolution rate can be converted to the dissolution half-life ($t_{1/2}$), expressed in hours, by using:

© 2024 The Author(s). Published by the Royal Society of Chemistry

Open Access Article. Published on 08 December 2023. Downloaded on 2/2/2024 12:01:41 PM.
This article is licensed under a Creative Commons Attribution-NonCommercial 3.0 Unported Licence.

$$t_{1/2} = \frac{\ln(2)}{\mathrm{BET} \times K_{\mathrm{dis}}} \quad (4)$$

The values of $t_{1/2}$ that are reported in the work refer to the first sampling from the intestine phase at $\Delta t = 155$ minutes total incubation time (Int_1).

4.5 Statistical analysis

Data are expressed as mean values ± standard deviation. Differences have been considered significant for p values < 0.05. Statistical analysis was conducted using GraphPad Prism 8.4 (GraphPad Software Inc., La Jolla, CA, USA). An Unpair Student's t-test was performed.

4.6 Similarity algorithms

Two similarity algorithms were applied to the dissolution and half-life data, particularly the x-fold comparison as used in the ECETOC NanoApp[63,64] and a Bayesian likelihood-based assessment described by Tsiliki *et al.*,[65] in order to assess whether NFs are sufficiently similar for risk assessment purposes. The x-fold comparison is calculated as the ratio of dissolution values per pair of NFs, whereas the latter uses Bayes factor (BF) calculations to compare pairs of dissolution and half-life in order to quantify how similar they are. Both methods were consistent in scoring NF pairs;[51] however, the x-fold approach only considers relative changes in the dissolution data and does not take into account half-life information.

Data availability

The datasets used and/or analysed during the current study are available from the corresponding author on reasonable request.

Author contributions

L. D. C.: investigation, data curation, writing original draft; J. G. K.: investigation; L. L.: investigation; V. M.: investigation; F. L.: investigation; D. Ag S.: investigation; G. T.: investigation, methodology; A. G. O.: writing – review & editing; V. S.: conceptualization, writing – review & editing; W. W. and S. S: conceptualization, resources, formal analysis and methodology, writing – original draft.

Conflicts of interest

At the time of the study, JGK and WW were employees of BASF SE, a company producing nanomaterials. The other authors declare that they have no competing interests.

Acknowledgements

The authors would like to thank Dr F. Drago for the helpful technical assistance with ICP-OES (IIT), and Dr Svenja Seiffert for support with the ICPMS interpretation. This work is within the GRACIOUS project funded by the European Commission, Grant Agreement 760840.

References

1 S. Sabella, Impact of Bionanointeractions of Engineered Nanoparticles for Nanomedicine, *Nanotoxicology: Progress toward Nanomedicine*, ed. Monteiro-Riviere N. A. and Tran C. L., 2nd edn, 2014, pp. 21–36.
2 L. Di Cristo, A. G. Oomen, S. Dekkers, C. Moore, W. Rocchia, F. Murphy, H. J. Johnston, G. Janer, A. Haase and V. Stone, Grouping Hypotheses and an Integrated Approach to Testing and Assessment of Nanomaterials Following Oral Ingestion, *Nanomaterials*, 2021, **11**(10), 2623.
3 F. Murphy, S. Dekkers, H. Braakhuis, L. Ma-Hock, H. Johnston, G. Janer, L. di Cristo, S. Sabella, N. R. Jacobsen and A. G. Oomen, An Integrated Approach to Testing and Assessment of High Aspect Ratio Nanomaterials and Its Application for Grouping Based on a Common Mesothelioma Hazard, *NanoImpact*, 2021, **22**, 100314.
4 E. S. Committee, A. Hardy, D. Benford, T. Halldorsson, M. J. Jeger, H. K. Knutsen, S. More, H. Naegeli, H. Noteborn and C. Ockleford, Guidance on Risk Assessment of the Application of Nanoscience and Nanotechnologies in the Food and Feed Chain: Part 1, Human and Animal Health, *EFSA J.*, 2018, **16**(7), e05327.
5 ISO, *Nanotechnologies—Use and Application of Acellular in Vitro Tests and Methodologies to Assess Nanomaterial Biodurability*, ISO Geneva, Switzerland, 2017.
6 ECHA, *Appendix R.6–1 for Nanoforms Applicable to the Guidance on QSARs and Grouping of Chemicals*, ECHA-19-H-15-EN, 2019.
7 M.-L. Avramescu, P. E. Rasmussen, M. Chénier and H. D. Gardner, Influence of PH, Particle Size and Crystal Form on Dissolution Behaviour of Engineered Nanomaterials, *Environ. Sci. Pollut. Res.*, 2017, **24**(2), 1553–1564.
8 L. Voss, P. E. Saloga, V. Stock, L. Böhmert, A. Braeuning, A. F. Thünemann, A. Lampen and H. Sieg, Environmental Impact of ZnO Nanoparticles Evaluated by *in Vitro* Simulated Digestion, *ACS Appl. Nano Mater.*, 2019, **3**(1), 724–733.
9 Y. Li, K. Jiang, H. Cao, M. Yuan and F. Xu, Influences of a Standardized Food Matrix and Gastrointestinal Fluids on the Physicochemical Properties of Titanium Dioxide Nanoparticles, *RSC Adv.*, 2021, **11**(19), 11568–11582.
10 H. M. Braakhuis, F. Murphy, L. Ma-Hock, S. Dekkers, J. Keller, A. G. Oomen and V. Stone, An Integrated Approach to Testing and Assessment to Support Grouping and Read-Across of Nanomaterials After Inhalation Exposure, *Appl. In Vitro Toxicol.*, 2021, **7**(3), 112–128.
11 V. Stone, S. Gottardo, E. A. Bleeker, H. Braakhuis, S. Dekkers, T. Fernandes, A. Haase, N. Hunt, D. Hristozov and P. Jantunen, A Framework for Grouping and Read-across of Nanomaterials-Supporting Innovation and Risk Assessment, *Nano Today*, 2020, **35**, 100941.
12 L. Di Cristo, V. C. Ude, G. Tsiliki, G. Tatulli, A. Romaldini, F. Murphy, W. Wohlleben, A. G. Oomen, P. P. Pompa and

© 2024 The Author(s). Published by the Royal Society of Chemistry

Open Access Article. Published on 08 December 2023. Downloaded on 2/2/2024 12:01:41 PM. This article is licensed under a Creative Commons Attribution-NonCommercial 3.0 Unported Licence.

J. Arts, Grouping of Orally Ingested Silica Nanomaterials *via* Use of an Integrated Approach to Testing and Assessment to Streamline Risk Assessment, *Part. Fibre Toxicol.*, 2022, **19**(1), 1–26.

13 L. Di Cristo, G. Janer, S. Dekkers, M. Boyles, A. Giusti, J. G. Keller, W. Wohlleben, H. Braakhuis, L. Ma-Hock and A. G. Oomen, Integrated Approaches to Testing and Assessment for Grouping Nanomaterials Following Dermal Exposure, *Nanotoxicology*, 2022, **16**(3), 310–332.

14 F. A. Murphy, H. J. Johnston, S. Dekkers, E. A. Bleeker, A. G. Oomen, T. F. Fernandes, K. Rasmussen, P. Jantunen, H. Rauscher and N. Hunt, How to Formulate Hypotheses and IATAs to Support Grouping and Read-across of Nanoforms, *ALTEX-Alternatives to Animal Experimentation*, 2023, **40**(1), 125–140.

15 J. B. Dressman, K. Thelen and E. Jantratid, Towards Quantitative Prediction of Oral Drug Absorption, *Clin. Pharmacokinet.*, 2008, **47**, 655–667.

16 M. R. Marques, R. Loebenberg and M. Almukainzi, Simulated Biological Fluids with Possible Application in Dissolution Testing, *Dissolution Technol.*, 2011, **18**(3), 15–28.

17 A. Brodkorb, L. Egger, M. Alminger, P. Alvito, R. Assunção, S. Ballance, T. Bohn, C. Bourlieu-Lacanal, R. Boutrou and F. Carrière, INFOGEST Static *in Vitro* Simulation of Gastrointestinal Food Digestion, *Nat. Protoc.*, 2019, **14**(4), 991–1014.

18 P. Bove, M. A. Malvindi, S. S. Kote, R. Bertorelli, M. Summa and S. Sabella, Dissolution Test for Risk Assessment of Nanoparticles: A Pilot Study, *Nanoscale*, 2017, **9**(19), 6315–6326.

19 C. Carnovale, D. Guarnieri, L. Di Cristo, I. De Angelis, G. Veronesi, A. Scarpellini, M. A. Malvindi, F. Barone, P. P. Pompa and S. Sabella, Biotransformation of Silver Nanoparticles into Oro-Gastrointestinal Tract by Integrated *in Vitro* Testing Assay: Generation of Exposure-Dependent Physical Descriptors for Nanomaterial Grouping, *Nanomaterials*, 2021, **11**(6), 1587.

20 D. Guarnieri, P. Sánchez-Moreno, A. E. Del Rio Castillo, F. Bonaccorso, F. Gatto, G. Bardi, C. Martín, E. Vázquez, T. Catelani and S. Sabella, Biotransformation and Biological Interaction of Graphene and Graphene Oxide during Simulated Oral Ingestion, *Small*, 2018, **14**(24), 1800227.

21 A. Mittag, A. Singer, C. Hoera, M. Westermann, A. Kämpfe and M. Glei, Impact of *in Vitro* Digested Zinc Oxide Nanoparticles on Intestinal Model Systems, *Part. Fibre Toxicol.*, 2022, **19**(1), 39, DOI: **10.1186/s12989-022-00479-6**.

22 I. S. Sohal, Y. K. Cho, K. S. O'Fallon, P. Gaines, P. Demokritou and D. Bello, Dissolution Behavior and Biodurability of Ingested Engineered Nanomaterials in the Gastrointestinal Environment, *ACS Nano*, 2018, **12**(8), 8115–8128.

23 H. Sieg, C. Kästner, B. Krause, T. Meyer, A. Burel, L. Böhmert, D. Lichtenstein, H. Jungnickel, J. Tentschert and P. Laux, Impact of an Artificial Digestion Procedure on Aluminum-Containing Nanomaterials, *Langmuir*, 2017, **33**(40), 10726–10735.

24 A. P. Walczak, R. Fokkink, R. Peters, P. Tromp, Z. E. Herrera Rivera, I. M. Rietjens, P. J. Hendriksen and H. Bouwmeester, Behaviour of Silver Nanoparticles and Silver Ions in an *in Vitro* Human Gastrointestinal Digestion Model, *Nanotoxicology*, 2012, **7**(7), 1198–1210.

25 F. N. Christensen, S. S. Davis, J. G. Hardy, M. J. Taylor, D. R. Whalley and C. G. Wilson, The Use of Gamma Scintigraphy to Follow the Gastrointestinal Transit of Pharmaceutical Formulations, *J. Pharm. Pharmacol.*, 1985, **37**(2), 91–95.

26 C. Jiménez-Arroyo, A. Tamargo, N. Molinero, J. J. Reinosa, V. Alcolea-Rodriguez, R. Portela, M. A. Bañares, J. F. Fernández and M. V. Moreno-Arribas, Simulated Gastrointestinal Digestion of Polylactic Acid (PLA) Biodegradable Microplastics and Their Interaction with the Gut Microbiota, *Sci. Total Environ.*, 2023, **902**, 166003.

27 W. Utembe, K. Potgieter, A. B. Stefaniak and M. Gulumian, Dissolution and Biodurability: Important Parameters Needed for Risk Assessment of Nanomaterials, *Part. Fibre Toxicol.*, 2015, **12**, 1–12.

28 N. Hunt, *Guidance on the GRACIOUS Framework for Grouping and Read-Across of Nanomaterials and Nanoforms*, (1.0)[WWW Document], Zenodo, 2021.

29 L. Traas and R. Vanhauten, *GRACIOUS Framework Blueprint*, 2021.

30 C. Peyrot des Gachons and P. A. Breslin, Salivary Amylase: Digestion and Metabolic Syndrome, *Curr. Diabetes Rep.*, 2016, **16**(10), 1–7.

31 R. A. Pouliot, B. M. Young, P. A. Link, H. E. Park, A. R. Kahn, K. Shankar, M. B. Schneck, D. J. Weiss and R. L. Heise, Porcine Lung-Derived Extracellular Matrix Hydrogel Properties Are Dependent on Pepsin Digestion Time, *Tissue Eng., Part C*, 2020, **26**(6), 332–346.

32 J. Ahn, M.-J. Cao, Y. Q. Yu and J. R. Engen, Accessing the Reproducibility and Specificity of Pepsin and Other Aspartic Proteases, *Biochim. Biophys. Acta, Proteins Proteomics*, 2013, **1834**(6), 1222–1229.

33 M. Mukherjee, Human Digestive and Metabolic Lipases—a Brief Review, *J. Mol. Catal. B: Enzym.*, 2003, **22**(5–6), 369–376.

34 E. Bauer, S. Jakob and R. Mosenthin, Principles of Physiology of Lipid Digestion, *Asian-Australas. J. Anim. Sci.*, 2005, **18**(2), 282–295.

35 A. F. Hofmann and K. J. Mysels, Bile Salts as Biological Surfactants, *Colloids Surf.*, 1987, **30**(1), 145–173.

36 R. Peters, E. Kramer, A. G. Oomen, Z. E. Herrera Rivera, G. Oegema, P. C. Tromp, R. Fokkink, A. Rietveld, H. J. Marvin and S. Weigel, Presence of Nano-Sized Silica during *in Vitro* Digestion of Foods Containing Silica as a Food Additive, *ACS Nano*, 2012, **6**(3), 2441–2451.

37 C. Singh, S. Friedrichs, M. Levin, R. Birkedal, K. A. Jensen, G. Pojana, W. Wohlleben, S. Schulte, K. Wiench and T. Turney, *NM-series of Representative Manufactured Nanomaterials: Zinc Oxide NM-110, NM-111, NM-112, NM-113 Characterisation and Test Item Preparation*, EUR 25066 EN-2011, 2011.

© 2024 The Author(s). Published by the Royal Society of Chemistry

Open Access Article. Published on 08 December 2023. Downloaded on 2/2/2024 12:01:41 PM. This article is licensed under a Creative Commons Attribution-NonCommercial 3.0 Unported Licence.

38 J. Estrada-Urbina, A. Cruz-Alonso, M. Santander-González, A. Méndez-Albores and A. Vázquez-Durán, Nanoscale Zinc Oxide Particles for Improving the Physiological and Sanitary Quality of a Mexican Landrace of Red Maize, *Nanomaterials*, 2018, **8**(4), 247.

39 M. E. Conrad, J. N. Umbreit and E. G. Moore, A Role for Mucin in the Absorption of Inorganic Iron and Other Metal Cations: A Study in Rats, *Gastroenterology*, 1991, **100**(1), 129–136.

40 A. Kathiravan, G. Paramaguru and R. Renganathan, Study on the Binding of Colloidal Zinc Oxide Nanoparticles with Bovine Serum Albumin, *J. Mol. Struct.*, 2009, **934**(1–3), 129–137.

41 P. Zhou, M. Guo and X. Cui, Effect of Food on Orally-Ingested Titanium Dioxide and Zinc Oxide Nanoparticle Behaviors in Simulated Digestive Tract, *Chemosphere*, 2021, **268**, 128843.

42 J. G. Keller, M. Persson, P. Mueller, L. Ma-Hock, K. Werle, J. Arts, R. Landsiedel and W. Wohlleben, Variation in Dissolution Behavior among Different Nanoforms and Its Implication for Grouping Approaches in Inhalation Toxicity, *NanoImpact*, 2021, **23**, 100341.

43 EFSA, Re-Evaluation of Silicon Dioxide (E 551) as a Food Additive, *EFSA J.*, 2018, **16**(1), e05088.

44 P. Laux, T. Tralau, J. Tentschert, A. Blume, S. Al Dahouk, W. Bäumler, E. Bernstein, B. Bocca, A. Alimonti and H. Colebrook, A Medical-Toxicological View of Tattooing, *Lancet*, 2016, **387**(10016), 395–402.

45 U. G. Sauer and R. Kreiling, The Grouping and Assessment Strategy for Organic Pigments (GRAPE): Scientific Evidence to Facilitate Regulatory Decision-Making, *Regul. Toxicol. Pharmacol.*, 2019, **109**, 104501.

46 H. Stratmann, M. Hellmund, U. Veith, N. End and W. Teubner, Indicators for Lack of Systemic Availability of Organic Pigments, *Regul. Toxicol. Pharmacol.*, 2020, **115**, 104719.

47 W. H. De Jong, E. De Rijk, A. Bonetto, W. Wohlleben, V. Stone, A. Brunelli, E. Badetti, A. Marcomini, I. Gosens and F. R. Cassee, Toxicity of Copper Oxide and Basic Copper Carbonate Nanoparticles after Short-Term Oral Exposure in Rats, *Nanotoxicology*, 2019, **13**(1), 50–72.

48 B. C. Krause, F. L. Kriegel, D. Rosenkranz, N. Dreiack, J. Tentschert, H. Jungnickel, P. Jalili, V. Fessard, P. Laux and A. Luch, Aluminum and Aluminum Oxide Nanomaterials Uptake after Oral Exposure-a Comparative Study, *Sci. Rep.*, 2020, **10**(1), 1–10.

49 H. Stratmann, W. Wohlleben, M. Wiemann, A. Vennemann, N. End, U. Veith, L. Ma-Hock and R. Landsiedel, Classes of Organic Pigments Meet Tentative PSLT Criteria and Lack Toxicity in Short-Term Inhalation Studies, *Regul. Toxicol. Pharmacol.*, 2021, **124**, 104988.

50 N. Jeliazkova, L. Ma-Hock, G. Janer, H. Stratmann and W. Wohlleben, Possibilities to Group Nanomaterials across Different Substances–a Case Study on Organic Pigments, *NanoImpact*, 2022, **26**, 100391.

51 N. Jeliazkova, E. Bleeker, R. Cross, A. Haase, G. Janer, W. Peijnenburg, M. Pink, H. Rauscher, C. Svendsen and G. Tsiliki, How Can We Justify Grouping of Nanoforms for Hazard Assessment? Concepts and Tools to Quantify Similarity, *NanoImpact*, 2022, **25**, 100366.

52 N. Boisa, N. Elom, J. R. Dean, M. E. Deary, G. Bird and J. A. Entwistle, Development and Application of an Inhalation Bioaccessibility Method (IBM) for Lead in the PM10 Size Fraction of Soil, *Environ. Int.*, 2014, **70**, 132–142.

53 E. Innes, H. H. Yiu, P. McLean, W. Brown and M. Boyles, Simulated Biological Fluids–a Systematic Review of Their Biological Relevance and Use in Relation to Inhalation Toxicology of Particles and Fibres, *Crit. Rev. Toxicol.*, 2021, **51**(3), 217–248.

54 I. Zanoni, J. G. Keller, U. G. Sauer, P. Müller, L. Ma-Hock, K. A. Jensen, A. L. Costa and W. Wohlleben, Dissolution Rate of Nanomaterials Determined by Ions and Particle Size under Lysosomal Conditions: Contributions to Standardization of Simulant Fluids and Analytical Methods, *Chem. Res. Toxicol.*, 2022, **35**(6), 963–980.

55 W. J. Peijnenburg, E. Ruggiero, M. Boyles, F. Murphy, V. Stone, D. A. Elam, K. Werle and W. Wohlleben, A Method to Assess the Relevance of Nanomaterial Dissolution during Reactivity Testing, *Materials*, 2020, **13**(10), 2235.

56 C. H. Versantvoort, A. G. Oomen, E. Van de Kamp, C. J. Rompelberg and A. J. Sips, Applicability of an *in Vitro* Digestion Model in Assessing the Bioaccessibility of Mycotoxins from Food, *Food Chem. Toxicol.*, 2005, **43**(1), 31–40.

57 A. G. Oomen, C. J. M. Rompelberg, M. A. Bruil, C. J. G. Dobbe, D. Pereboom and A. Sips, Development of an *in Vitro* Digestion Model for Estimating the Bioaccessibility of Soil Contaminants, *Arch. Environ. Contam. Toxicol.*, 2003, **44**(3), 0281–0287.

58 V. Marassi, L. Di Cristo, S. G. Smith, S. Ortelli, M. Blosi, A. L. Costa, P. Reschiglian, Y. Volkov and A. Prina-Mello, Silver Nanoparticles as a Medical Device in Healthcare Settings: A Five-Step Approach for Candidate Screening of Coating Agents, *R. Soc. Open Sci.*, 2018, **5**(1), 171113.

59 V. Marassi, S. Casolari, S. Panzavolta, F. Bonvicini, G. A. Gentilomi, S. Giordani, A. Zattoni, P. Reschiglian and B. Roda, Synthesis Monitoring, Characterization and Cleanup of Ag-Polydopamine Nanoparticles Used as Antibacterial Agents with Field-Flow Fractionation, *Antibiotics*, 2022, **11**(3), 358.

60 J. G. Keller, W. Peijnenburg, K. Werle, R. Landsiedel and W. Wohlleben, Understanding Dissolution Rates *via* Continuous Flow Systems with Physiologically Relevant Metal Ion Saturation in Lysosome, *Nanomaterials*, 2020, **10**(2), 311.

61 J. G. Keller, U. M. Graham, J. Koltermann-Jülly, R. Gelein, L. Ma-Hock, R. Landsiedel, M. Wiemann, G. Oberdörster, A. Elder and W. Wohlleben, Predicting Dissolution and Transformation of Inhaled Nanoparticles in the Lung Using Abiotic Flow Cells: The Case of Barium Sulfate, *Sci. Rep.*, 2020, **10**(1), 1–15.

62 J. Koltermann-Jülly, J. G. Keller, A. Vennemann, K. Werle, P. Müller, L. Ma-Hock, R. Landsiedel, M. Wiemann and

 © 2024 The Author(s). Published by the Royal Society of Chemistry

Open Access Article. Published on 08 December 2023. Downloaded on 2/2/2024 12:01:41 PM.
This article is licensed under a Creative Commons Attribution-NonCommercial 3.0 Unported Licence.

W. Wohlleben, Abiotic Dissolution Rates of 24 (Nano) Forms of 6 Substances Compared to Macrophage-Assisted Dissolution and *in Vivo* Pulmonary Clearance: Grouping by Biodissolution and Transformation, *NanoImpact*, 2018, **12**, 29–41.

63 G. Janer, R. Landsiedel and W. Wohlleben, Rationale and Decision Rules behind the ECETOC NanoApp to Support Registration of Sets of Similar Nanoforms within REACH, *Nanotoxicology*, 2021, **15**(2), 145–166.

64 G. Janer, D. Ag-Seleci, J.-A. Sergent, R. Landsiedel and W. Wohlleben, Creating Sets of Similar Nanoforms with the ECETOC NanoApp: Real-Life Case Studies, *Nanotoxicology*, 2021, **15**(8), 1016–1034.

65 G. Tsiliki, D. A. Seleci, A. Zabeo, G. Basei, D. Hristozov, N. Jeliazkova, M. Boyles, F. Murphy, W. Peijnenburg and W. Wohlleben, Bayesian Based Similarity Assessment of Nanomaterials to Inform Grouping, *NanoImpact*, 2022, **25**, 100389.